APPLICATION OF ULTRAFILTRATION AND NANOFILTRATION PROCESSES IN PETROLEUM INDUSTRY

A THESIS SUBMITTED TO
THE GRADUATE SCHOOL OF NATURAL AND APPLIED SCIENCES
OF
MIDDLE EAST TECHNICAL UNIVERSITY

BY

IŞIN DİZVAY

IN PARTIAL FULFILLMENT OF THE REQUIREMENTS
FOR
THE DEGREE OF MASTER OF SCIENCE
IN
CHEMICAL ENGINEERING

FEBRUARY 2022

Approval of the thesis:

APPLICATION OF ULTRAFILTRATION AND NANOFILTRATION PROCESSES IN PETROLEUM INDUSTRY

submitted by **IŞIN DİZVAY** in partial fulfillment of the requirements for the degree of **Master of Science** i**n Chemical Engineering, Middle East Technical University** by,

Prof. Dr. Halil Kalıpçılar
Dean, Graduate School of **Natural and Applied Sciences** _____

Prof. Dr. Pınar Çalık
Head of the Department, **Chemical Engineering** _____

Assoc. Prof. Dr. Zeynep Çulfaz Emecen
Supervisor, **Chemical Engineering, METU** _____

Examining Committee Members:

Prof. Dr. Ülkü Yetiş
Environmental Engineering, METU _____

Assoc. Prof. Dr. Zeynep Çulfaz Emecen
Chemical Engineering, METU _____

Prof. Dr. Levent Yılmaz
Chemical Engineering, METU _____

Assoc. Prof. Dr. Berna TOPUZ
Chemical Engineering, Ankara Uni. _____

Asst. Prof. Dr. Emre Büküşoğlu
Chemical Engineering, METU _____

Date: 11.02.2022

I hereby declare that all information in this document has been obtained and presented in accordance with academic rules and ethical conduct. I also declare that, as required by these rules and conduct, I have fully cited and referenced all material and results that are not original to this work.

Name Last name : Işın Dizvay

Signature :

ABSTRACT

APPLICATION OF ULTRAFILTRATION AND NANOFILTRATION PROCESSES IN PETROLEUM INDUSTRY

Dizvay, Işın
Master of Science, Chemical Engineering
Supervisor : Assoc. Prof. Dr. Zeynep Çulfaz Emecen

February 2022, 79 pages

Membrane separations become prominent as green techology is taking over. Besides many traditional separation processes being replaced with membrane applications, many potentials are discovered to be transformed. Petrochemical industry is one of the fields with many potentials. This study includes two different membrane applications on different processes in petrochemical industry.

Vast amount of produced water from oil fields requires a number of separation processes to be disposed properly or to be reused. As an economic and environmental alternative, membrane separations have been used for a while. Yet, membrane replacement is inevitable due to the fouling. The first part of this study focuses on anti fouling strategies on polyethersulfone (PES) hollow fiber membranes during oil-water emulsion (OWE) filtrations. OWE was filtered on hollow fiber membranes in a cross-flow system at pressures starting from 0,3 bar, at 0,2 bar increments until limiting flux is reached.The effect of hollow fiber geometry, cross-flow velocity, emulsion type and membrane material on fouling were observed. Spiral fiber geometry has a superiority over standart tubular geometry with respect to fouling.

Also, cross-flow velocity was found to be reversely related to fouling. More hydrophilic cellulose acetate (CA) membrane fouled less and more reversibly than PES membrane. Emulsion oil droplet size distrubution and oil-surfactant constituents in the emulsions also affected the fouling reversibility.

The second part of the studyis on ethylene glycol recovery from a petrochemical stream. Recovery and recycle of organic compounds are necessary in industry due to economic and environmental reasons. Ethylene glycol (EG) is a commercial product as a part of the ethylene oxide production process. A stream containing EG and $NaHCO_3$ was treated to separate $NaHCO_3$ from EG. In order to do this, 3 commercial nanofiltration (NF) membrane (Desal DK, DL, HL) performances were observed in a cross-flow system. It was found that a stream containing 2,2 % $NaHCO_3$ and 2,5 % EG can be desalinated to 0,22 % $NaHCO_3$ and 2,5 % EG with a two stage process using Desal DK membrane.

Keywords: Oil-Water Emulsion, Antifouling, Hydrodynamics, EG, $NaHCO_3$

ÖZ

PETROL ENDÜSTRİSİNDE ULTRAFİLTRASYON VE NANOFİLTRASYON PROSES UYGULAMALARI

Dizvay, Işın
Yüksek Lisans, Kimya Mühendisliği
Tez Yöneticisi: Doç. Dr. Zeynep Çulfaz Emecen

Şubat 2022, 79 sayfa

Çevreci teknolojinin ön plana çıkmasıyla membran prosesleri göze çarpar hale geldi. Geleneksel ayırma proseslerinin membran uygulamalarıyla değiştirilmesinin yanında, ihtimal dahilinde olabilecek prosesler de değerlendirilip membran prosesleriyle değiştiriliyor. Petrokimya endustrisi bu açıdan bir çok potansiyel barındırmaktadır. Bu çalışma petrokimya endsutrisindeki iki proses icin membran uygulamalarını icermektedir.

Petrol sahalarından çıkarılan büyük miktardaki suyun, tekrar kullanılabilmesi ya da yönetmeliklere uygun bertaraf edilebilmesi icin bir çok ayırma işlemine tabi tutulması gerekmektedir. Membranla ayırma, ekonomik ve çevreci bir alternatif olarak bir süredir kullanılmaktadır. Yine de kirlenmeden dolayı, membran değişimi kaçınılmazdır. Bu çalışmanın ilk kısmı, PES'ten yapılmıs kovuklu elyaf membranların yağlı su emulsiyonu (OWE) filtrasyonu için anti-kirlenme stratejileri içermektedir. Kovuklu membranlarda OWE filtrasyonu, çapraz akış sisteminde, 0,3 bardan baslayıp 0,2 barlık artışlarla limit akışa ulaşana kadar devam ettirilerek yapılmıştır. Kovuklu elyaf membran geometrisi, çapraz akış hızı, emulsiyon çeşidi

ve membran malzemesinin kirlenme üzerindeki etkileri incelenmistir. Kirlenmeme açısından, spiral geometri, standart tüp geometrisine göre daha avantajlı bulunmuştur. Kirlenme, çapraz akış hızı ile ters orantılıdır. Daha hidrofilik olan seluloz asetattan yapılmış kovuklu elyaf membranın, PES'ten yapılmış olana göre daha az ve temizlenebilir şekilde kirlendiği görülmüştür. Emulsiyondaki damlacık boyut dağılımı ve yağ-yüzey aktif madde içerikleri de kirliliğin kalıcılığı üzerinde etkili olmuştur.

Çalısmanın ikinci kısmı, etilen glikolün petrokimyasal bir proses hattından geri kazanımı üzerinedir. Organik bileşiklerin geri kazanımı ve geri dönüşümü ekonomik ve çevresel nedenlerden dolayı endustride gereklidir. Etilen glikol (EG) etilen oksit üretimiyle bağlantılı oluşan ticari bir üründür. EG ve $NaHCO_3$ içeren bir proses hattı, $NaHCO_3$'ın EG'den ayrılması için işleme tabi tutulmuştur. Bunun için, 3 ticari nanofiltrasyon (NF) membranın (Desal DK, DL, HL) filtrasyon performansları çapraz akış sisteminde gözlenmiştir. 2,2 % $NaHCO_3$ ve 2,5 % EG içeren bir proses hattının içeriğinden, iki aşamalı Desal DK membran kullanılarak, 0,22 % $NaHCO_3$ ve 2,5 % EG elde edilebileceği bulunmuştur.

Anahtar Kelimeler: Yağ-Su Emulsiyonu, Antikirlilik, Hidrodinamik, EG, $NaHCO_3$

To my beloved family…

ACKNOWLEDGMENTS

I wish to express my deepest gratitude to my supervisor Assoc. Prof. Dr. Zeynep Çulfaz Emecen for her guidance, advice, criticism and insight throughout the research.

I would like to thank all of my lab mates Onur, Seden, Berk, Feyza, Toprak, Ceren, Ilker for making the lab time fly. It was especially precious being with them during the curfews.

Also, I am very thankful for having great officemates; Sılay and Ezgi, for letting me whine and making me feel not alone.

I would like to thank everyone especially 'badim Ilker', calling up during the late nights at the lab and making me feel safe and joyful after all.

I would like to thank Anıl for his friendship and for saving my day multiple times with his expertise.

I would like to express my deepest gratitude to my family; Ayse, Meral, Erdal and Sezin for believing in me and supporting me no matter what without any hesitation. I cannot be who I am today without them.

But, I cannot thank enough to my room mates and Tatom for making this challenging time fun, beautiful and worth to remember, and being there for me, owning every bit of this study as theirs. I feel so lucky having them in my life.

Finally, I would like to thank to Socar Turkiye for funding the second part of this study.

TABLE OF CONTENTS

LIST OF TABLES

TABLES

LIST OF FIGURES

FIGURES

LIST OF ABBREVIATIONS

ABBREVIATIONS

T80- Tween 80

OWE-Oil- water emulsion

HF- Hollow fiber

EG- Ethylene glycol

PES- Polyethersulfone

CA- Cellulose Acetate

NF- Nanofiltration

LIST OF SYMBOLS

SYMBOLS

R	Resistance
J	Permeate Flux
η	Permeate Viscosity
V	Permeate Volume
A	Active Membrane Area
$R_{membrane}$	Membrane Resistance
$R_{fouling}$	Fouling Resistance
k_c	Mass transfer coefficient
$\mathbb{R}_i\%$	% Rejection of Compound i
$C_{F,i}$	Feed Concentration of i in the Feed (or Retentate) Side
$C_{P,i}$	Permeate Concentration of i in the Permeate Side

CHAPTER 1

INTRODUCTION

Clean water is essential for all living things as well as industrial processes. However, with the industrialization, water contamination and global warming disturbing the hydrologic cycle, water scarcity is upon us. Wastewater recycle is not just an ecofriendly process anymore, but it is a need as in desalination of seawater. Until several measures become effective in water crisis, reuse of water is inevitable. Even though many conventional processes contribute to the reuse of water, the separation technology used in conventional processes demands high energy and additional chemicals. Fortunately, there are cleaner, energy-saving alternatives to the conventional separation processes.

A membrane separates species depending on the size of the molecules and chemical/physical interaction between the molecules and the membrane. It allows the transport of some species through while retaining others, or controls the rate of permeation of different species, thereby achieving separation between species.

A usual classification of membranes is made with respect to membrane pore size given in Figure 1.1.

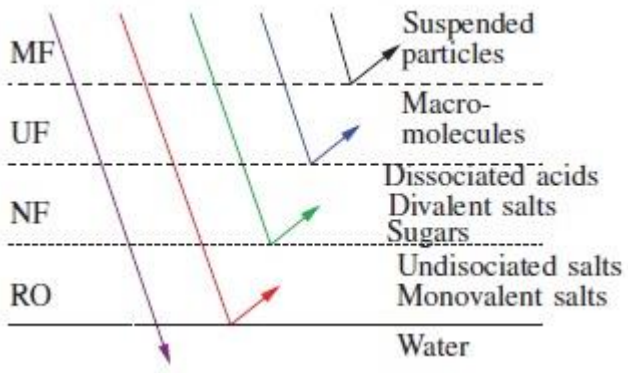

Figure 1.1 Membrane Classification. (Fikar, 2014)

Microfiltration (MF) membranes separate suspended particles larger than their pore size. MF membranes have pore size in the range of 0.1 and 10 μm. The feed side of the membrane is pressurized so that the smaller molecules pass through the membrane while larger particles are retained. Ultrafiltration (UF) differs by the pore size from MF. UF membrane pore size varies between 10-100 nm. Since the pore size in UF is smaller than MF, the applied pressure increases accordingly to provide the flow. UF focuses on the macromolecules. MF and UF operate according to the same transport mechanism, pore flow. Permeate is carried away with the convective flow resulted from the pressure applied on the feed side of the membrane. Pore size determines the extent of separation via size exclusion.

Among the pressure-driven classes of membranes, reverse osmosis (RO) has a different separation mechanism than MF and UF. RO membranes separate solutes that are not dissolved in the membrane material. Dissolved solutes diffuse according to the concentration gradient along RO membrane. Thus, the permeate is transported according to the solution-diffusion mechanism. Nanofiltration,(NF) on the other hand, is a class defined later. NF is a transition region between UF and RO. The pore size is in the range of 1-2 nm. However, the working principle differs from UF and MF by the charge exclusion mechanism in addition to size exclusion. A NF membrane not only sieves the molecules but also has the ability to repel/attract a molecule due to its charge. NF is usually made of polymers with a charged group on

its back bone. So that, the membrane surface becomes charged and separates molecules accordingly. It requires less pressure applied compared to RO, and retains small molecules better than UF with a reasonable flux. Neutral molecules smaller than 1 nm cannot be separated by NF. Since, NF rejects molecules according to Donnan exclusion, it is commonly used for multivalent ion separation as a pretreatment step for RO in desalination process or as a part of wastewater treatment process. The transport mechanism of each NF membrane depends on its structure. If it lies closer to UF region, pore flow model applies in the transport of molecules, but solution-diffusion model leads the transport mechanism if it is closer to RO region. (Baker, 2001)

The membranes are incorporated into a process by 2 modes. The fluid is fed perpendicularly to the membrane by the pressure applied on the feed side of the membrane in the dead-end filtration mode. A basic expression of dead-end filtration is given in Figure 1.2. Molecules bigger than the pore size concentrate on the membrane during filtration.

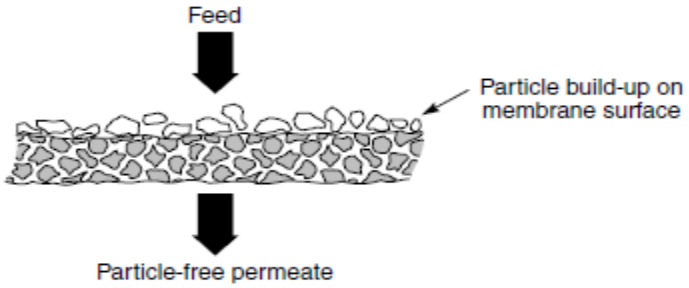

Figure 1.2 Dead-end Filtration (Baker, 2001)

Besides dead-end mode, cross-flow filtration mode, as shown in Figure 1.3, is commonly used. The flow across the surface prevents the retained molecules from depositing on the surface, while applied pressure provides a flow through the membrane. The purified stream is called permeate, and the concentrated stream is called retentate.

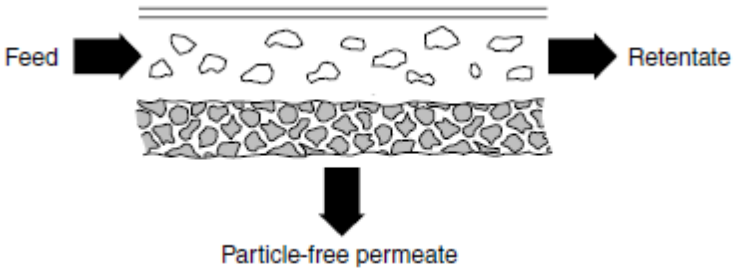

Figure 1.3 Cross-flow Filtration (Baker, 2001)

Membrane fouling is a result of the physical and chemical interactions between colloidal particles, solutes and the membrane surface. This interaction may result in adsorption or deposition of the particles on the surface or in the pores of the membrane causing flux decline. Fouling of a membrane can be explained by Figure 1.4. Before the solution filtration, membrane's pure water permeance is measured by permeating water. Permeate flux of a virgin membrane depends on the characteristics of the membrane such as pore size and porosity of the membrane and trans membrane pressure applied. In the 2nd region, permeate flux decline is observed due to the partial/full blockage of the pores or cake formation by the solute during its filtration. After a physical cleaning step between regions II and III, permeate flux is typically seen to recover partially during water filtration in region III. The flux decline is a result of 2 types of fouling. The recovered part of flux with simple cleaning (water flush or back wash) is caused from reversible fouling while the rest of the flux that cannot be recovered is a result of irreversible fouling. Usually, irreversible fouling is eliminated by harsher methods such as chemical treatments.

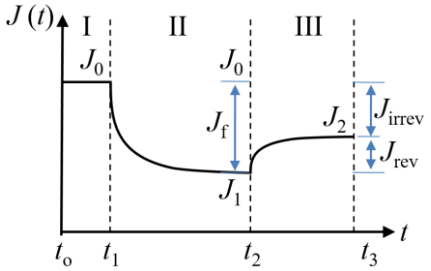

Figure 1.4 Permeate flux during pure water filtration (I), solution filtration (II) and pure water filtration again (III) (Huang et al., 2018)

CHAPTER 2

LITERATURE REVIEW

In petrochemical industry, separation is a crucial step regarding the cost and the final product. Membrane separation is an attractive alternative for the conventional separation units due to its simplicity and low energy requirement. Waste streams in petrochemical industry may contain toxic compounds to be disposed as well as reactants to be recycled and reused. Moreover, industrial and produced water can be reused in many processes after pretreatments. Membrane separations enable the reuse of toxic and/or valuable chemicals and save water.

2.1 Oily Water Treatment with Membranes

2.1.1 Oily Water

Daily oil production has reported to be 88 million barrels worldwide in 2020 according to BP Statistical Review of World Energy 2021. It is known that an average of 3 barrels of water is produced for every barrel of oil (Liang et al., 2018). Thus, 270 million barrels of produced water (PW) is needed to be reinjected, treated or disposed daily. However, this vast amount of PW contains oil and many contaminants that have limits to dispose among regulations. The components of PW from oil fields are given in Table 2.1. it should be noted that the content of the PW varies field to field due to its geological characteristics, reservoir life time, how it is produced, etc.

Table 2.1 Produced water constituents from oil fields (Liang et al., 2018)

Parameter	**Range (mg/L)**	**Parameter**	**Range (mg/L)**
Aluminum	310-410	Manganese	0.004-175
Ammoniacal nitrogen	10-300	Mercury	0.001-0.002
Arsenic	0.005-0.3	Phenols	0.009-23
Barium	1.3-650	Potassium	24-4300
Beryllium	0.001-0.004	Silver	0.001-0.15
Bicarbonate	77-3990	Sodium	132-97000
Boron	5-95	Strontium	0.02-1000
Cadmium	0.005-0.2	Sulfate	2-1650
Calcium	13-25800	Sulfite	10
Chemical oxygen demand	1220	Titanium	0.01-0.7
Chloride	80-200000	Total organic carbon (TOC)	0-1500
Chromium	0.02-1.1	Total oil	2-565
Copper	0.002-1.5	Total polar	9.7-600
Higher acids	1-63	Total suspended solids (TSS)	1.2-1000
Iron	0.1-100	Volatile	0.39-35
Lead	0.002-8.8	Volatile fatty acids	2-4900
Lithium	3-50	Zinc	0.01-35
Magnesium	8-6000		

Even though the constitents of PW differ from the other oily wastewater constituents, treatment for different oil types varies slightly. Oily wastewater, in general, contains oil in 2 forms; free oil that can float on the water and dispersed oil that is found in

the dispersed phase, water. However, if dispersed oil is stabilized in the presence of a surfactant, it is called emulsion, otherwise droplets in the dispersed form may coalesce and starts to float as free oil form. Floating and dispersed oil require different treatment methods. (Huang et al., 2018) Treatment method is determined according to the oil droplet size distribution. (Benyahia et al., 2016). While conventional methods are suitable to separate floating oils, they are insufficient on the emulsions due to oil droplet size (<10 μm) and having comparable density with water. (Huang et al., 2018)

Treatment ofoily wastewater requires sophisticated methods that focus on components such as TSS, TOC, dissolved oil, traces of elements, etc. Initially, compounds with density differences are separated such as solid particles, hydrocarbon compounds having lower density than water. This step includes gravity separators in various forms. In the second step, dissolved components are aimed to be separated. Large and small oil droplets are eliminated by flotation method; biodegradable organics are consumed by microorganisms; and various pore sizes of membranes are also employed for different compounds. Microfiltration membrane is responsible for the retention of suspended solids and compounds causing turbidity. Ultrafiltration membrane is used to filter dissolved macromolecules and suspended colloidal particles. Since nanofiltration membranes are tighter than UF and MF, the task is to eliminate color, volatile organic compounds, multivalent ions. Reverse osmosis membrane rejects almost all ionic species and dissolved solutes. The 3rd step is required for lowering organics, turbidity, nitrogen phosphorus, metals and pathogens via oxidation and degradation techniques. (Olajire, 2020)

2.1.2 Membrane Fouling

Fouling behavior varies depending on the foulant. Foulants are classified into 4 types;

- Non-migratory foulants (organic colloids, natural organic matters, biomacromolecules)
- Spreadable foulants (typically, oil)
- Biofoulants (living organisms)
- Inorganic foulants (fully / partially precipitated salts). (Zhao et al., 2018)

Oil droplets, as spreadable foulant, have their own fouling mechanism due to their coalescence and deformation shown in Figure 2.1. In the beginning of a filtration of oil water emulsion, oil droplets drifted with the permeate flow accumulate on the membrane surface causing a partial blockage (a) and decline in the permeate flux. As the emulsion filtration continues, more oil droplets placing on the membrane surface form a cake layer (b). Also, in cross- flow filtration, oil droplets tend to adrift with the cross-flow. Thus, cake layer becomes permanent as the balance between the accumulated and drifted away oil droplet is reached. Since oil droplets can be deformed easily and they have tendency to coalesce, the cake layer becomes resistant to water flow. Even though the cake layer becomes resistant with the coalescence of droplets, it is also possible that the bigger droplets forming via coalescence are prone to get drifted with the cross-flow. Due to the applied pressure, coalesced droplets spread on the membrane surface in the form of a film (c). Contiguous film formation on the membrane is more common for underwater oleophilic membranes, and requires more serious actions than cake layer does. Those 3 cases are valid for the droplets that do not fit in the pores of the membrane. Whereas, droplets that can fit or relatively comparable in size with the pore size of the membrane may accumulate within the pores due to adsorption (d). Internal fouling is also hard to clean. (Huang et al., 2018)

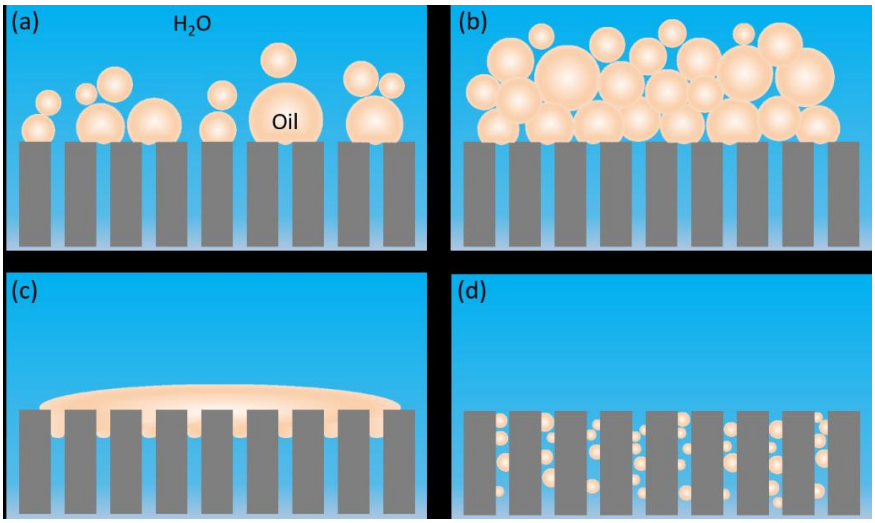

Figure 2.1 Oil fouling models in oil water emulsion filtration; a) partial blockage, b) cake layer formation, c) contiguous oil film, d) oil droplets within the pores. (Huang et al., 2018)

2.1.2.1 Membrane Materials

Antifouling membranes are the milestones in making membrane applications widespread. Since fouling is related to the interactions between membrane and foulant of the system, it is essential to choose membrane material accordingly. Some factors depending on the feed, such as pH, concentration, temperature, or hydrodynamic conditions are not feasible to be adjusted due to the process parameters, however, membrane material selection may overcome with those harsh conditions.

So, each membrane process application requires a particular material selection with respect to hydrophilic/hydrophobic property, MWCO, pore size and distribution. These are the main characteristics that interaction between the foulant and membrane depends on. Properties such as MWCO, pore size and distribution can be set during the fabrication of the membrane.

First of all, hydrophilic property is known to resist fouling. A hydrophilic surface has fewer hydrophobic sites for foulant adhesion. (Fane et al., 2006) In fact, a hydrophilic surface has hydrogen-bond acceptors that attaches a thin layer of water on the surface of the membrane and provides a barrier to foulant adhesion. (Singh, 2015) But, hydrophilic material is not the only solution to have a hydrophilic surface. In fact, the addition of hydrophilic groups into a hydrophobic material is more preferable due to the mechanical and thermal stability of the hydrophobic materials. A variety of commercial membranes are cellulose, cellulose acetate (CA) - hydrophilic, polypropylene (PP) and polyethylene (PE)-hydrophobic. Yet, polysulfone (PS) / polyethersulfone (PES), polyacrylontrile (PAN), and polyv inylidene fluoride (PVDF) are among the most used polymers. Despite their hydrophobicity, they are modified to provide a hydrophilic surface via blending with additives or surface post-modifications. (Pearce, 2007)

The durability of the membrane depends on the molecular weight of the polymer used. The higher the degree of polymerization, the tougher the material becomes. (Pearce, 2007). Also, it is crucial to be chlorine resistant for the membrane material in order to withstand chlorine disinfection. The temperature and pH endurance of the material should be matched up with the operating temperature and pH.

After considering the parameters mentioned above, it is also inevitable to continue with a cost effective material selection especially for the large scale applications. The main commercial polymer products are made of PS, CA, PP, PES and PVDF. (Pearce, 2007)

In this study, PES is decided to be the main membrane material for its robustness and slight hydrophilicity. The modification of PES surface can be done with the addition of sulfone, carboxyl, hydroxyl, and amine functional groups for hydrophilic property via physical adsorption, UV irradiation, plasma treatment, blending method or bulk modification. (Alenazi et al., 2017)

2.1.2.2 Effect of Operation Conditions

Each membrane unit is designed for a specific feed. Even though the temperature, pressure and the constituents of the feed can be adjusted according to the efficiency of the process, the design criteria mainly focus on the operating conditions. The operating conditions of a membrane process are temperature, cross flow velocity, trans membrane pressure and permeate recovery. However, operating conditions are especially important in membrane separation due to the fouling of the membrane. In order to prolong the life of the membrane, it is essential to operate under optimal conditions.

To start with, fluid viscosity is indirectly proportional to temperature. Thus, an increase in the temperature causes a decrease in the viscosity of the fluid and that increases the permeate flux. (Gorouhi et al., 2006), (Hu & Scott, 2008)

But, its effect on the membrane fouling is not as clear as its effect on the permeate flux. Emulsion stability increases with temperature as a result of decrease in the surface tension yielding smaller oil droplets. However, with the increase in temperature, surfactants may also leave the oil-water interface causing oil droplet coalescence. (Chen & Tao, 2005)

Moreover, filtration mode contributes to fouling. In most of the large-scale processes, cross-flow has an obvious advantage over dead-end configuration. In cross-flow configuration, droplets follow the main flow, across the membrane surface, whereas, in dead-end configuration, oil droplets are pushed against the membrane surface with the applied pressure. (Huang et al., 2018)

In addition to the superiority of the cross-flow configuration, it is important to determine the optimal cross-flow velocity. Since, the rejected oil droplets accumulate around the membrane surface causing concentration polarization. Lobo et al. found that increasing cross-flow velocity increases permeate flux due to the

formation of turbulence in the flow. Turbulence disrupt the oil droplets accumulating on the membrane surface. (Lobo et al., 2006)

Regarding oil-water separation processes, internal fouling is caused by oil droplets pressed into the pores. Thus, the maximum trans membrane pressure should not exceed the critical pressure that required for the oil droplet entering a pore. (Monfared et al., 2016)

2.1.2.3 Effect of Turbulance

As mentioned before, in order to prevent concentration polarization, mass transfer boundary layer near the membrane wall should be disturbed. Some of the common methods are static turbulence promoter i.e. static mixer, pulsed flow, centrifugal instability creation in flow, i.e Dean vortices, helical baffle, vibrating membranes, etc. (Vatai et al., 2007)

Um et al. tried nitrogen gas injection to increase permeate flux. With the optimal conditions of gas fraction in feed and gas bubble size were arranged, it was found that gas injection creates turbulance and decreases concentration polarization of 5% cutting oil-water emulsion. Permeate flux increased due to turbulance created. Specifically, the flux increased to 400% of the no gas injection flux when the emulsion concentration factor was 5. (Um et al., 2001)

A static mixer usage was proved to eliminate concentration polarization and fouling on a zirconia membrane with a 5% cutting oil emulsion by Krstic et al. Not only static mixer use improved permeate flux by at least 100% depending on the feed flow rate, but also, it resulted in a lower specific energy consumption.

In addition to turbulence effect, Dean vortices are known to adjust the hydrodynamics by a coiled tube. Dean vortices are created as a result of the geometry of the tube where the flow is placed. Flow in a curved channel creates Dean vortices. Thus, it does not require additional energy as in pulsed flow, that, Dean

vortices are provided by the design of the membrane channel with its helical structure. During a flow in a coiled tube, secondary flows are observed due to the centrifugal forces. Dean number determines if the flow pattern changes and vortices are observed. Dean number is defined as;

$$De = Re\sqrt{\frac{di}{dc}} \quad (1)$$

Re- Reynolds number

di- inside diameter of the fiber

dc-effective coil diameter

Effective coil diameter can be defined via Figure 2.2.

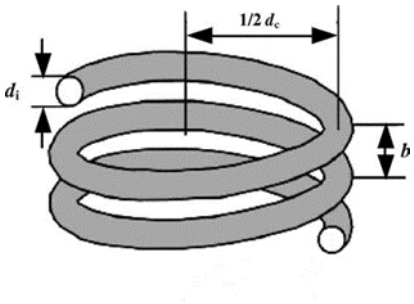

Figure 2.2 Dean vortices in a coiled channel (Liu et al., 2005)

Therefore, dc can be found as below,

$$dc = dh\left[1 + \left(\frac{b}{\Pi\ dh}\right)^2\right] \quad (2)$$

dh- helix diameter

b- pitch of the coil

To sum up, membrane fouling during the oil separation from produced water is inevitable. There are many parameters that contribute to fouling. Such as, membrane material selection due to the interactions between the membrane and the foulant. Or, operational conditions such as temperature, pressure, filtration mode. Also, there are parameters to be adjusted to mitigate fouling, i.e cross-flow velocity, use of static turbulance promoters. Thus, the parameters affecting fouling should be adjusted to prevent fouling.

2.2 Organic/Salt Separation with NF

Organic compounds are recovered via high-energy energy consuming processes such as distillation and evaporation due to their extensive use in many industries. The reuse of organics is required for environmental concerns and cost minimization. Also, regulations upon organic waste disposal requires organic compounds to be separated from discharge water. Membrane applications have advantages in organics separation compared to the conventional methods.

In many cases, the streams aimed to recover the organic content contain salt at high concentrations. In order to recover organic compounds for reuse, separation process to retain either the salts or the organic compound in the mixture needs to be arranged. NF membranes are strong candidates for their separation mechanism. Organic compounds over ca. 1 nm or 200 g/mol are retained by NF, whereas a remarkable amount of salts are retained due to their charge. (Kim et al., 2006)

Commercial NF membranes, UTC-20, Desal-HL-51, NTR-7450, NF270 and NF-PES-010, were subjected to various organic compounds (tryptophane, raffinose, benzylidene acetone and mandelic acid) in order to see the separation mechanism in a study by Braeken et al. Filtrations were performed at various pH to observe the pH effect on the charge of the membrane and solutions, and the rejection of the compounds. Mandelic acid was rejected higher than 80% by all membranes due to

negative charges of the molecule and membrane at a pH of 10. Whereas its rejection by all membranes was lower at acidic pH, since mandelic acid was partially ionized and the membranes were positively charged. Similarly, the rejection of benzylidene acetone was below 20% by all membranes at a pH of 10, since the molecule was neutral at that pH and it was a small molecule to be sieved. UTC-20, Desal-HL-51 and NF270 rejected tryptophane over 80% at all pH. While NTR-7450 and NF-PES-010 had lower rejection values. That can be explained by sieving of the tryptophane molecule because tryptophane is zwitterionic, thus has no net charge when dissolved. High retention-membranes had lower MWCO than tryptophane, and low retention-membranes had higher MWCO than tryptophane. Raffinose is bigger in size compared to the other molecules, thus rejected better than others by all membranes. When these results were considered, it was seen that both Donnan exclusion and sieving contributed to separation. (Braeken et al., 2006)

Yoon et al. examined the rejection mechanism of various organic and inorganic compounds on commercial RO and NF membranes. The organic compounds were creatine, 2-(2-Butoxyethoxy) ethanol, caprolactam, 2-Propanol, formaldehyde, methanol, urea and inorganic compounds were ammonium carbonate and sodium chloride. Even though rejection by size exclusion is considered to be a function of molecular weight, it was found that creatine (MW131.2 g/mol) was rejected 96% by RO (AK) and LPRO (ESPA) membranes, the rejection of 2-(2-butoxyethoxy) ethanol (BEE) (MW 162.2 g/mol) was only 80% by the same membranes. The higher rejection for the lower molecular weight-molecule was explained by the solute radius of the molecules. Creatine has a solute radius of 0,37 nm whereas BEE's solute radius is 0,32 explaining the higher rejection of creatine despite of its lower molecular weight. Among the organic compounds, urea, formaldehyde and methanol were rejected by 15-20% which can be explained by being uncharged and small molecules. However, the rejection of 2-propanol was significantly higher than urea which has the same molecular weight (60,1 g/mol) with. Once more, this was a result of solute radius effect. (Yoon & Lueptow, 2005)

The effect of salt concentration on the retention of organic compounds was investigated by Luo et al. Commercial NF polymeric membranes, NF270, NF-, Desal-5 DL and Nanomax50, were first subjected to 2 g/l glucose solutions. It was found that the solution permeance values were as high as the pure water permeance showing that 2 g/l glucose solution was diluted enough so that concentration polarization was negligible. NF270 and NF- membranes showed higher rejection than Desal-5 DL and Nanomax50 due to their lower molecular weight cut-off (MWCO). The salt concentration effect was observed via 15 g/l glucose solution with NaCl concentrations varying from 0 to 3 M. Even for the mere 15 g/l glucose solution, flux decline was observed due to the concentration polarization. With increasing salt concentration, decline in the permeate flux was observed. That might be caused from either salt ions increased the water viscosity in the pores, or salt concentration increased the bulk fluid viscosity that back diffusion of glucose mitigated resulting in concentration polarization of glucose. The obvious salt concentration effect on glucose rejection was noticed for all membranes. (Luo & Wan, 2011)

NF was studied as an alternative for purification step in lactic acid production process by Bouchoux et al. 2 streams were subjected to DK NF membrane. The 1st stream contained lactate ions with Cl^-, $H_2PO_4^-$, SO_4^{2-}, Na^+, K^+, Ca^{2+} and Mg^{2+}. Lactate ion carried along with Na^+ in permeate, thus showed a similar rejection with Na^+, around 22%. K^+, a similar sized and charged ion, retained 18%. Divalent ions, Ca^{2+}, Mg^{2+}, SO_4^{2-}, PO_4^{3-} were rejected higher compared to the other ions. Yet, lactate purification was not significant due to the presence of Na^+ and K^+ ions in the permeate. In the 2nd stream lactic acid, a neutral molecule, was present with Cl^-, $H_2PO_4^-$, SO_4^{2-} and Na^+. Lactic acid was recovered due to its lack of charge and smaller size compared to the DK membrane pore size. SO_4^{2-} and PO_4^{3-} were rejected by around 50% due to their size and charge. Still, partial purification of neutral organic molecules was found successful in regards to multivalent ions. (Bouchoux et al., 2006)

Ethylene glycol is included as a raw material in the production process of many daily materials such as clothes, pillows, jet skis, bathtubs, and bowling balls, packaging film and bottles depending on its form. Beside its anti-freeze usage, it is commonly used as a heat transfer agent. Due to its widely use, EG has been listed in top ten pollutants, thus it's crucial to recover EG from waste streams. (Biancari et al., 2003) Waste streams i.e. from PET production and from EG production can be recovered to prevent pollution and for the reuse of EG. (Biancari et al., 2003)

Specifically,the common production process of EG involves the hydrolysis of ethylene oxide patented by Shell (Harmsen & Verkerk, 2020). This process is a 2 stage process, starting with the production of ethylene oxide. Then, in the glycol step, EG is formed as a result of ethylene oxide and water reaction. However, ethylene oxide also reacts with products forming diethylene glycol (DEG), triethylene glycol (TEG), and heavier glycols as byproducts. The amount of byproducts is limited to 10% by adjusting water to ethylene oxide feed ratio. But, the excess amount of water has to be removed from the product by evaporation. DEG and TEG are separated from EG by distillation. CO_2 produced as a product from the reaction between ethylene-O_2 competing with the main reaction between ethylene and O_2. CO_2 is removed by the reaction with an aqueous alkali metal carbonate solution (K_2CO_3 or Na_2CO_3). As a result of this reaction, $KHCO_3$ or $NaHCO_3$ is added to the ethylene oxide-containing streams fed to EG production unit. A general scheme of the process is given in Figure 2.3.

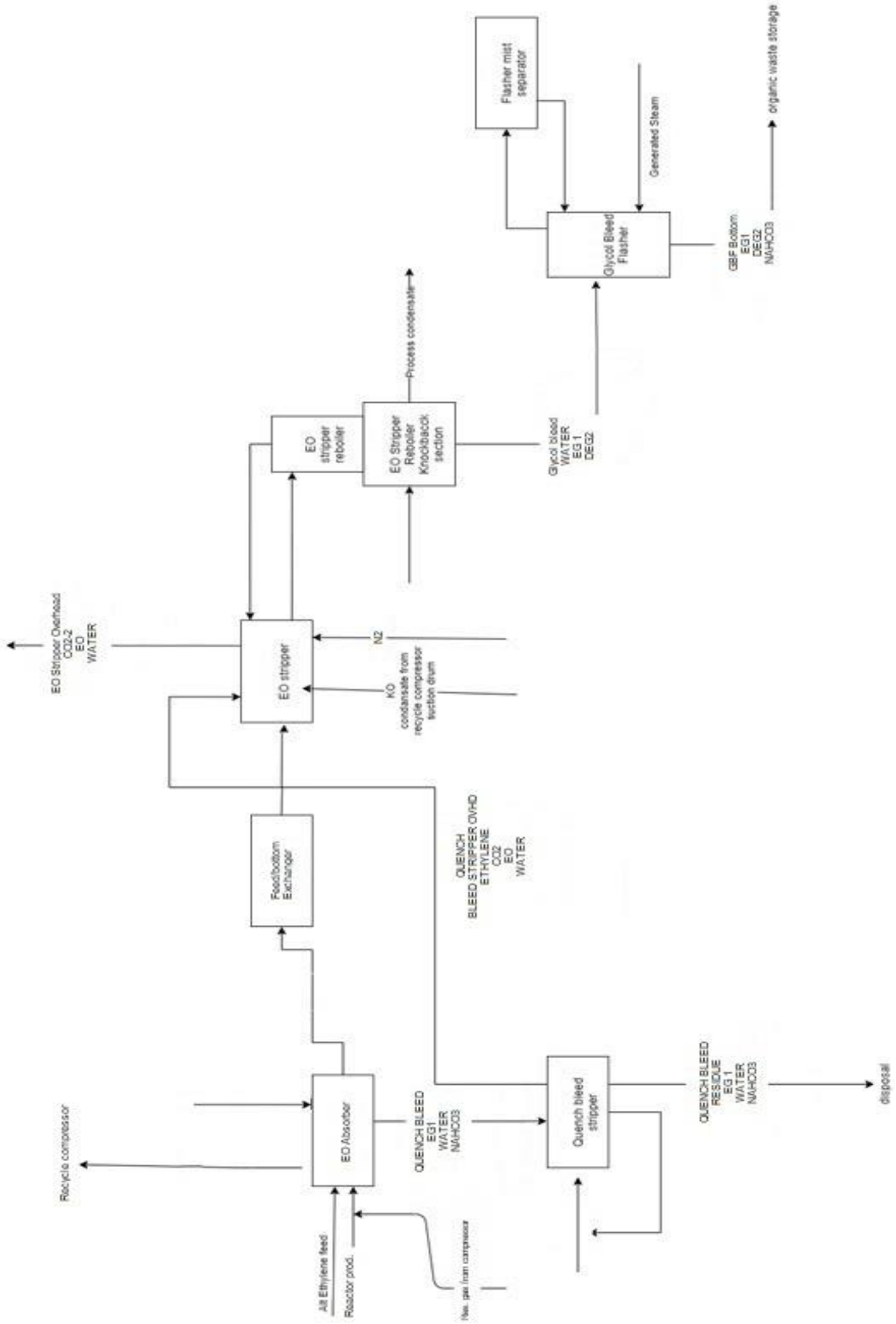

Figure 2.3 Ethylene Oxide/Ethylene Glycol production process

Streams containing reasonable amount of EG can sometimes be sent to waste because of the salt content. The disposal of those streams is hard because of its organic and salt content. With proper treatments, a secondary grade EG can be provided. Thus, the main aim of this study is to retain salt from the EG concentrated streams to achieve a secondary grade EG.

Nanofiltration membranes can be a good option with their looser (compared to RO) and charged structure (compared to UF) to allow a better flux yet a selective performance. Nanofiltration membranes are known to reject salts depending on the size and the charge. Even though, the size of the ion is small enough to pass through the membrane, its charge may not allow it. The Donnan exclusion mechanism is a result of the charged groups on the membrane polymer's backbone. Since the same charged ions with the membrane are repelled and opposite charges are attracted, the concentration of the same –charged ions are lower in the membrane phase than in bulk phase and counter ion concentration is higher in the membrane phase than in the bulk phase. Donnan potential, the potential difference at the interphase, pulls the counter ions while repelling the same-charged ions.

2.3 Aim of the Study

This study aims to investigate oil-water separation for produced water and EG recovery from $NaHCO_3$ containing aqueous solution via membrane separations.

To start with, traditional methods has been replaced by membrane processes for oil-water separations for a while. However, the major drawback of membrane applications for oil-water separation is membrane fouling. Industrial and oil field-produced water has already been treated by membranes to follow the disposal and reuse regulations. Usually, MF and UF applications have proven that the separation performance is sufficient. The cost compared to the traditional methods has been

lower in membrane separations. Even so, membrane fouling requires chemical/physical cleaning or use of a fresh membrane. Oil fouling and anti fouling coatings are hot topics concerning the problem. This study investigates the effects of hydrodynamic parameters, material and emulsion effects on the fouling. In order to observe the effect of the fiber geometry, straight and helical hollow fibers are used. Moreover, filtrations at different Reynolds numbers are conducted. Spiral geometry and increase in the cross-flow velocity are known to increase the shear rate on the membrane surface and are expected to result in lower fouling. A more hydrophlic membrane material is also used to observe the material effect on the fouling. Lastly, emulsions with various oil and surfactants are prepared and filtered to observe the fouling for each case. Among three emulsion recipes, vegetable oil-water recipe was used as a control factor in the experiments. Vegetable oil was selected due to the reproducibility of the emulsions with the same oil droplet size distribution.

In addition to the oil-water emulsion separations, it is aimed to separate $NaHCO_3$ from EG containing aqueous solution. EG is a product of EO and water reaction, and it is a highly chemical and a toxic substance to dispose without precautions. Many applications in petrochemical industry for chemical substance recovery has been widely common. However, EG recovery has not been investigated in the literature. Separation of organic compounds has been examined through membrane filtration. In a similar sense, NF can be used to separate $NaHCO_3$ from EG, so a set of commercial NF membranes are tested with respect to separation performances.

CHAPTER 3

EXPERIMENTAL METHODS

3.1 Oily Water Treatment

3.1.1 Materials

PES (Ultrason E6020P) was provided by BASF. Before use, PES was put in 80 ^{0}C vacum oven for one night at atmospheric pressure. N-methyl pyrrolidone (NMP, %99) was purchased from Sigma-Aldrich which was used as solvent for PES. Carrefour brand sun flower oil was purchaed from supermarket. Tween 80, a non-ionic surfactant, and sodium dodecyl sulfate (SDS), an anionic surfactant, (≥ 99%) were purchased from Sigma Aldrich. A commercial boron oil with specifications given below was used.

Table 3.1 Boron oil specifications

Density, g/cm^3, 15°C	0,89
Kin. Viscosity, mm^2/s, 40°C	25,05
pH (Emulsion), 20 ºC	9
Color Concentrate/Emulsion	Yellow/Milk white

Membrane performance experiments modules were prepared by using epoxy solution which contains REN HY 5160 and RENLAM CY 219 both were purchased from RenShape Solutions. Ultrapure water (UP) (18.3 mΩ.cm) was used to prepare

feed solutions for filtration experiments and at physical membrane cleaning procedures.

3.1.2 Membrane Fabrication

3.1.2.1 Flat Sheet Membranes

Flat sheet membranes are fabricated from PES. Pre-dried PES is dissolved in NMP (n-methyl-2-pyrrolidone) by keeping the solution on the roller mixer for 1-2 days. After being homogenized, the solution is cast with a 250 μm-thickness casting bar. Cast membranes are immersed in the UP water bath for 10 minutes for the coagulation step of the phase inversion method. To remove remaining NMP in the membrane, the membrane is placed in RO water containing beaker for an hour and then for 24 hours with refreshed RO water. Fabricated flat sheet membranes are kept in 20% ethanol solution until their use.

3.1.2.2 Hollow Fiber

The hollow fibers were fabricated by Hazal Yucel by spinning. (Yücel & Çulfaz-Emecen, 2018). PES solutions are prepared as described in Section 3.1.2.1. PES solution for the hollow fibers is composed of 15.3% PES, 5.1% Triton 100X, 72.3% NMP and 7.3% UP water. The spinning process parameters varied accordingly for twisted and straight hollow fibers used in this study. Flow rates of polymer dope and bore liquid were 11.48 and 3.45 mL/min for twisted HF, 8.61 and 2.59 mL/min for straight HF. Coagulation bath temperture was set to 27º C for both fibers. Air gap was 6 and 4 cm for twisted and straight HFs, respectively.

Hollow fibers were made into modules for the performance tests. A 12 cm-piece hollow fiber was cut, and put in a 10-cm long plastic tube with a 4-cm diameter.

Then the ends of the tube were sealed with epoxy solution containing REN HY 5160 and RENLAM CY 219 as 1:2 weight ratio, respectively. The epoxy was cured approximately in 2 days.

3.1.3 Membrane Characterization

3.1.3.1 Scanning Electron Microscopy (SEM)

The cross-sections and shell and bore side morphologies of the hollow fibers are observed by SEM. The SEM images are taken by QUANTA 400F Field Emission SEM in METU Central Laboratory. The samples are frozen with liquid nitrogen and then broken to expose the cross-sectional area. The samples are kept in the vacuum overnight after all pieces are taped on the sample holders. Right before the analysis, the samples are coated with Au/Pd.

3.1.3.2 Attenuated Total Reflectance Fourier Transform Infrared Spectroscopy (ATR-FTIR)

In order to observe surfactant absorption on the surface of the membrane, FTIR analysis is used. IR-PRESTIGE-21 SCHIMADZU device in METU Chemical Engineering Department was used for the analysis. The resolution of the device is 1 cm^{-1}. The spectra of the samples were scanned from 4000 to 499 cm^{-1} wavenumber.

3.1.4 Solution-Emulsion Preparation

3.1.4.1 Surfactant Solution

Surfactant solution is used for the pretreatment of the membrane surface right before the OWE filtration. 600 ml of 0,1 g/l Tween 80 solution is stirred at 500 rpm for an hour.

3.1.4.2 Oil Water Emulsion Variations

Three different recipes used in the filtrations. The recipes are given in Table 3.2. All recipes were mixed in the stirrer to ensure that the maximum oil droplets' diameter are in the range of 5 μm.

Table 3.2 Oil-water emulsions

Recipe code	Oil/ Concentration	Surfactant/ Concentration	Stirring rate/ duration
OWE-Tween 80	Sunflower oil/ 1 g/l	Tween 80/ 0,1 g/l	1200 rpm/ 12 hours
OWE-SDS	Sunflower oil/ 1 g/l	SDS/ 0,07 g/l	700 rpm/ 10 hours
OWE-B	Boron oil/ 1 g/l	None*	300 rpm/ 6 hours

*Surfactant present in oil formulation

3.1.5 Droplet Size and Concentration Determination

3.1.5.1 Optical Microscopy

The emulsions were observed during the stirring via Zeiss Axio Scope A1 microscope. Filtration was started as soon as the intended oil droplet size was reached. Prepared emulsion images were taken for each filtration.

3.1.5.2 Dynamic Light Scattering (DLS)

DLS is used to measure the hydrodynamic diameters of the oil droplets in oil water emulsions. The analysis is conducted at room temperature via Malvern Zetasizer Nano in METU Chemical Engineering Department. The samples were analyzed at 13, 90 and 175^{o} angles three times. Each measurement was given in the plot. The samples analyzed were taken from the emulsions prepared for filtration, thus, samples were at the same concentration with the emulsions.

3.1.5.3 Turbidity Meter

The value of turbidity is a measure for oil presence in oil-water emulsions. Thus, feed, permeate and retantate samples were analyzed in turbidity meter for their oil concentration. Turbidity was measured using a HI 88703 laboratory turbidimeter. The device ranges from 0.00 to 9.99; 10.0 to 99.9; 100 to 4000 NTU with 0.01; 0.1; 1 NTU resolution. Four detectors measure at 90°, 180°, forward and backward scattering. A 5-point calibration was performed prior to each series of samples. Values were detected as a peak response between 400-600 nm. Measurements were taken in normal mode as recommended for stable emulsion samples and immediately after mixing. All measurements were done three times in NTU (ratio)-mode.

3.1.6 Membrane Performance Test

3.1.6.1 Pure Water Permeance (PWP)

Pure water permeance is measured in both batch mode (dead-end cell) and cross-flow mode. Regardless of the mode, PWP measurement is performed at 2 different trans membrane pressures (TMP), at 2 and 1 bar. Permeate is collected at 10-minute time intervals at constant pressure. Then, permeance, PWP, is calculated using the formula below;

$$PWP = \frac{J}{TMP} \tag{3}$$

where J referring to permeation flux (L/m^2.hr) and TMP referring to trans membrane pressure (bar).

3.1.6.2 Dead-end Filtrations

Dead-end filtrations were performed on flat PES membranes to decide whether surfactant was absorbed on the surface of the membrane. Filtrations were run in batch mode in 200 mL Amicon stirred cell at 200 rpm at 2 bar. 1 ml of surfactant solution/cm^2 membrane area was permeated. Pressure was maintained at 2 bar throughout the whole filtration via nitrogen in tank. After each filtration membrane surface is covered with water and stirred at 600 rpm for 10 minutes. Pure water permeance is measured before and after each filtration using UP water.

3.1.6.3 Cross-flow Filtrations

Cross-flow mode was the main filtration mode used for the hollow fiber membranes. A Watson Marlow 505s pump was used to control the flow rate thus the cross-flow velocity. A back-pressure valve was used to regulate the flow rate and pressure of the retantate. A cross-flow velocity was determined and the pump and the back pressure valve opening were set to a value accordingly. Then, feed was given to the system via the pump. A manometer connected prior to membrane module measured the inlet pressure of the system. Feed flows between the tube and the hollow fiber, permeated from outside to inside of the membrane. The back-pressure valve was connected between the membrane module and retantate tube. Retantate and permeate were recycled to the feed tank, so that the feed concentration was kept constant. A schematic of the system is given in Figure 3.1.

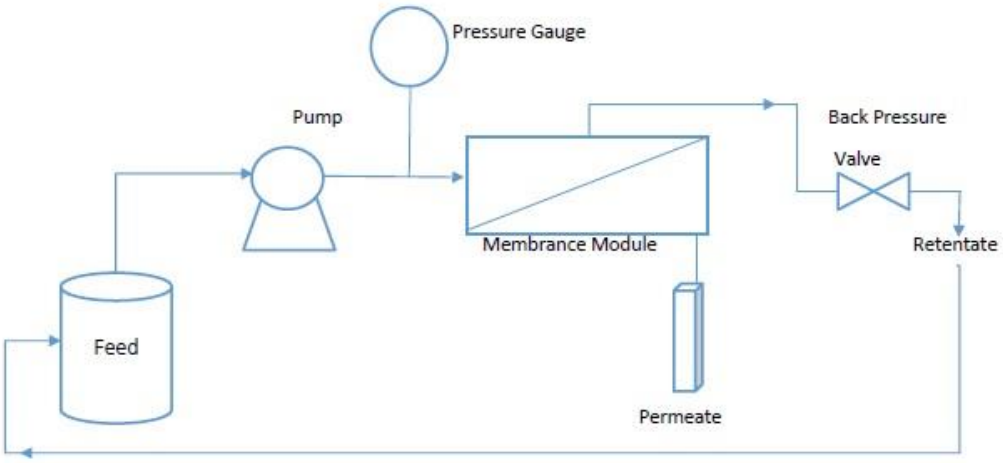

Figure 3.1 Schematic of the cross-flow system

Surfactant solution filtration mentioned in previous section were performed on hollow fiber membranes in cross-flow mode at 192,5 ml/min cross-flow velocity.

Pressure was kept at 1,5 bar throughout the whole filtration via the back-pressure valve. 1 ml of surfactant solution/cm^2 membrane area was permeated.

OWE filtrations were performed at increasing TMP starting from 0,3 bar to 1,7-1,9 bar. Pressure was regulated via the back-pressure valve starting from 0,3 bar, increased by 0,2 bar for each cycle. The pump was set to provide a Reynolds number of 400, 970 and 1485. For the filtration from outside of the fiber to the inside of it, module hydraulic diameter, D_h, is calculated as follows;

$$Dh = Dt - Do \tag{4}$$

where D_t is the tube diameter and D_o is the outside diameter of the fiber.

The system was run in the full recycle mode, thus, the permeate was collected and its flow rate was measured for a certain pressure setting and then returned to the feed tank when a new pressure was adjusted. Permeance is calculated by using the equation (6) and resistance of membrane (Rm) and fouling (Rf) can be calculated as below;

$$R = \frac{TMP}{ŋ.J} \tag{5}$$

$$R = Rm + Rf \tag{6}$$

where

R- Total resistance, m-1

ŋ- Permeate viscosity, Pa.s

J- Flux during filtration, L/m2.bar.

Resistance of the membrane, Rm, depends only on the membrane itself. Thus, it is calculated according to the pure water flux value via equation (5). However, the total resistance, R, is calculated according to a solution filtration flux value, and calculated

via equation (5). The difference between R and Rm, Rf, is the fouling from the solution.

The membrane is subjected to PWP measurements before and after each filtration, so that the effect of fouling on the permeance of the membrane can be observed. The permeance of pure water loss, PWP loss%, caused by fouling is calculated as below,

$$PWP\ loss\ \% = 100x\left(\frac{PWP\ after\ surfactant\ treatment - PWP\ after\ filtration}{PWP\ after\ surfactant\ treatment}\right) \quad (7)$$

In equation (7) calculation, PWP value after the surfactant treatment is counted as the base value. Before measuring PWP after filtration, the membrane surface was swept with UP water without any pressure applied after each filtration.

The separation performance of the membrane is evaluated according to equation (8) given below.

$$\mathbb{R}(\%) = 100x\left(1 - \frac{cp}{cf}\right) \quad (8)$$

where

$\mathbb{R}$- Rejection of the foulant (oil)

c_p- concentration of the foulant in the permeate

c_f- concentration of the foulant in the feed

3.2 EG Recovery from Aqueous EG- $NaHCO_3$ Solutions

3.2.1 Materials

Ethylene glycol (≥ 99,5%) and $NaHCO_3$ (≥ 99,7%) used for the feed solutions were supplied from Merck. The NF membranes used in the filtrations were Suez brand. The specifications of the membranes are given below.

Table 3.3 Membrane specifications provided by Suez

	DK	**DL**	**HL**
pH Range	2-10	2-10	
Flux (GFD)/psi	22/100	31/100	39/100
MgSO4 Rejection	98%	96%	95%
MWCO	~150-300 Da	~150-300 Da	~150-300 Da
Polymer	Polyamide-TFC	Polyamide-TFC	Polyamide-TFC
Max. Pressure/ Temperature	40 bar/80ºC	40 bar/80ºC	40 bar/50ºC

Ultrapure water (UP) (18.3 mΩ.cm) was used to prepare feed solutions for filtration experiments and at physical membrane cleaning procedures.

3.2.2 Solution Preparation

The center of EG recovery project is the lines containing significant concentrations of EG in the presence of $NaHCO_3$. Thus, two different solutions of those streams were prepared with EG and salt concentrations given in Table 3.4.

Table 3.4 EG and salt concentrations of solutions

Stream #	**1**	**2**
EG concentration (% by mass)	26%	2,5%
Salt concentration (% by mass)	0,15%	2,2%

Before performing the filtration tests, solutions with only $NaHCO_3$ (0,15% and 2,2%) were filtered. After that, solutions were prepared containing both EG and salt.

For each filtration tests, 5 liters of solution was prepared. Then the beakers were put onto mixer, and mixed for 2 hours at 1000 rpm.

3.2.3 Performance Tests

3.2.3.1 Pure Water Permeance

PWP measurement was performed as described in Section 3.1.6.1. The operation TMP of DESAL DK, DL and HL membranes were 10-40 bar in this set up, so it was appropriate to measure PWP at 30, 20 and 10 bars.

3.2.3.2 Total Recycle Mode

Feed tank was filled the solution prepared. Feed, permeate, retentate and bypass tubes were all placed in the feed tank because feed solution concentration was aimed to be constant by not collecting permeate. The pump was started and let worked under no applied pressure for 5 minutes. Then pressure was set through retentate and bypass valves, accordingly. Retentate and permeate concentraions were examined via conductivity meter in every 20 minutes. Filtration ended after 3 hours. After the filtration ended by turning off the pump, the feed tank was emptied and filled with UP water and UP water was circulated through the system with no applied pressure

to clean the remainings in the system and on the membrane surface. Then, feed tank was refilled with fresh UP water to measure the pure water permeance.

3.2.3.3 Concentration Mode

Concentration mode differs from recycle mode by collecting the permeate. So, the feed was concentrated in time. Thus, all tubes except permeate tube were placed in feed tank, and permeate tube was placed in a separate tank. Filtration continued until 80% of feed volume was collected at least.

3.2.4 EG Concentration by TOC Analysis

EG in the feed, permeate and retentate was detected via TOC analysis. Total Organic Carbon analysis were performed at the METU- Chemical Engineering laboratories. A Shimadzu TOC-VCPH model TOC device performed analysis by "the 680°C combustion catalytic oxidation method". As the column catalyst platinum catalyst was used.

Samples drawn to the column are combusted under 680°C temperature and CO_2 detected in the infrared gas analyzer is recorded as Total Carbon (TC). For Inorganic Carbon (IC) analysis, samples are treated by acid in the device first, and then the organic compounds are digested and recorded as IC. The device obtains the TOC values by subtracting IC from TC.

3.2.5 $NaHCO_3$ Concentration by Conductivity Meter

A VWR brand conductivity meter was used to measure $NaHCO_3$ concentration in the feed, retentate and permeate samples. The device is capable of measuring the conductivity of any solution in the range of 0.01 µS/cm - 200.0 mS/cm with a

resolution of 0.01 μS/cm - 0.1 mS/cm upon selected range. Electrical conductivity is the measurement of the ion concentration in a sample. This is calculated by the ability of the substance to transmit an electrical current over a defined area. Thus, a range of samples was prepared fort the calibration curve. Then, every conductivity measurement was converted into the concentration data.

CHAPTER 4

RESULTS AND DISCUSSION

4.1 Oily Water Treatment

4.1.1 Membrane Morphology

The cross-sections and surface morphology of previously fabricated membranes were analyzed by SEM.

	Cross-section (250x)	Cross-section (1000x)	Shell side	Bore side
Helical HF	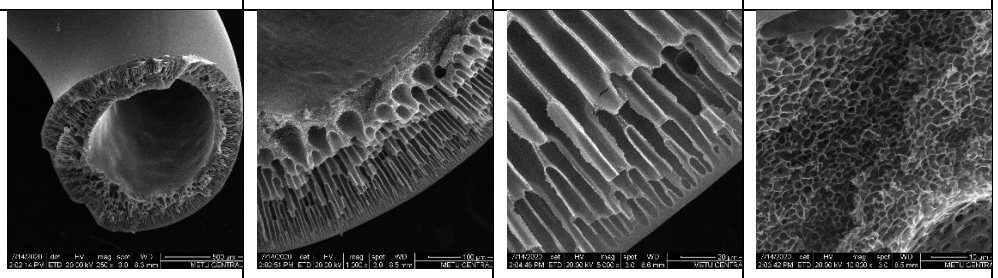			
Straight HF	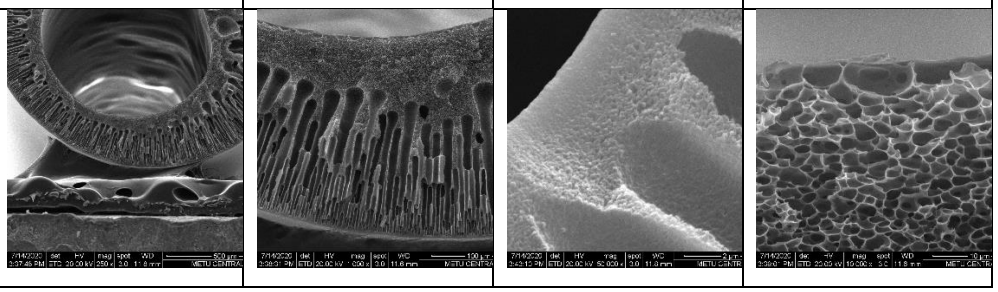			

Figure 4.1 SEM images of twisted and straight hollow fibers

Figure 4.1 shows that both helical and straight hollow fibers have skin on the shell side of the fibers. Other specifications of the hollow fiber membranes are given in Table 4.1.

Table 4.1 Hollow fiber specifications

Membr. Code	Geo.	Di (µm)	Do (µm)	Dhelix * (mm)	Pitch * (mm)
H72	Helical/twisted	561	1088	2.0	2.0
H77	Straight	635	1307	-	-

*Helix diameter and pitch of the coil are given in Figure 2.2.

Hollow fiber membranes placed in modules are seen as in Figure 4.2.

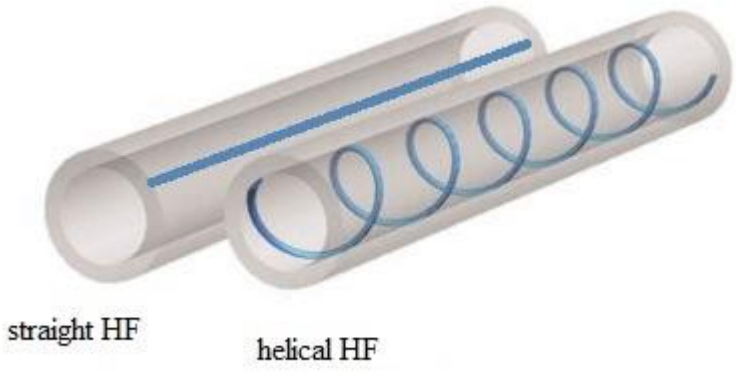

Figure 4.2 Image of a) straight hollow fiber and b) helical hollow fiber in module tubes

4.1.2 Droplet Size Determination

Oil droplet diameters were analyzed by DLS and optical microscopy. DLS analysis results and optical microscopy images are given in Figure 4.3 and 4.4, respectively. Each plot shows 3 out of 5 measurements made by DLS.

a)

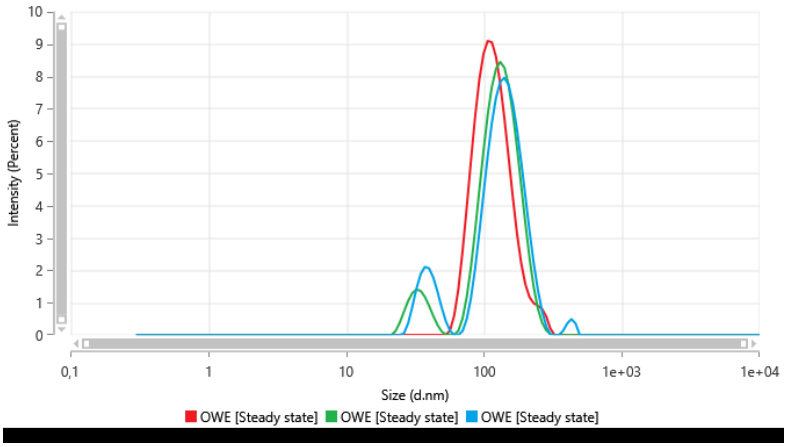

b)

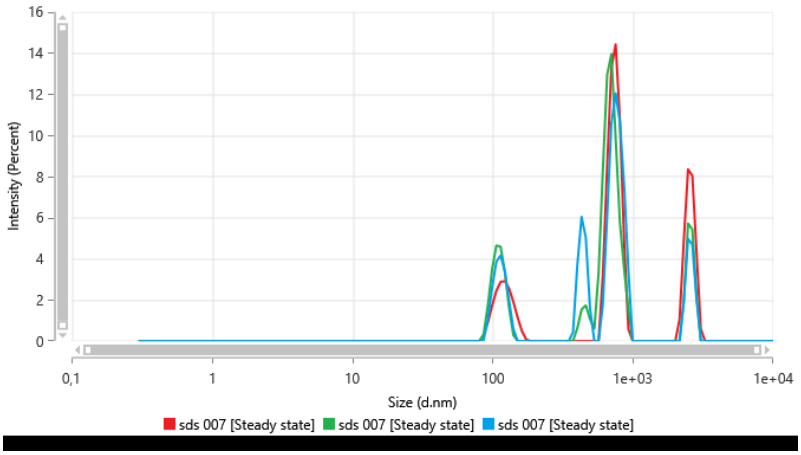

c)

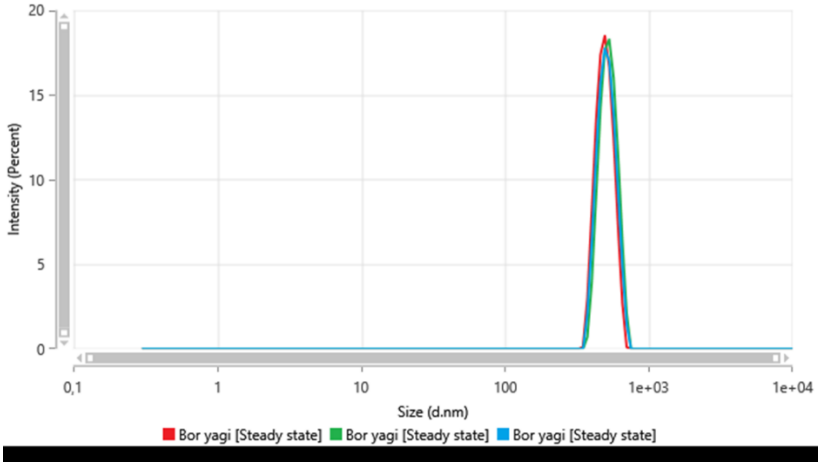

Figure 4.3 Oil droplet diameter results for a) OWE-T80, b) OWE-SDS, c) OWE-B via DLS, repeated three times

a)

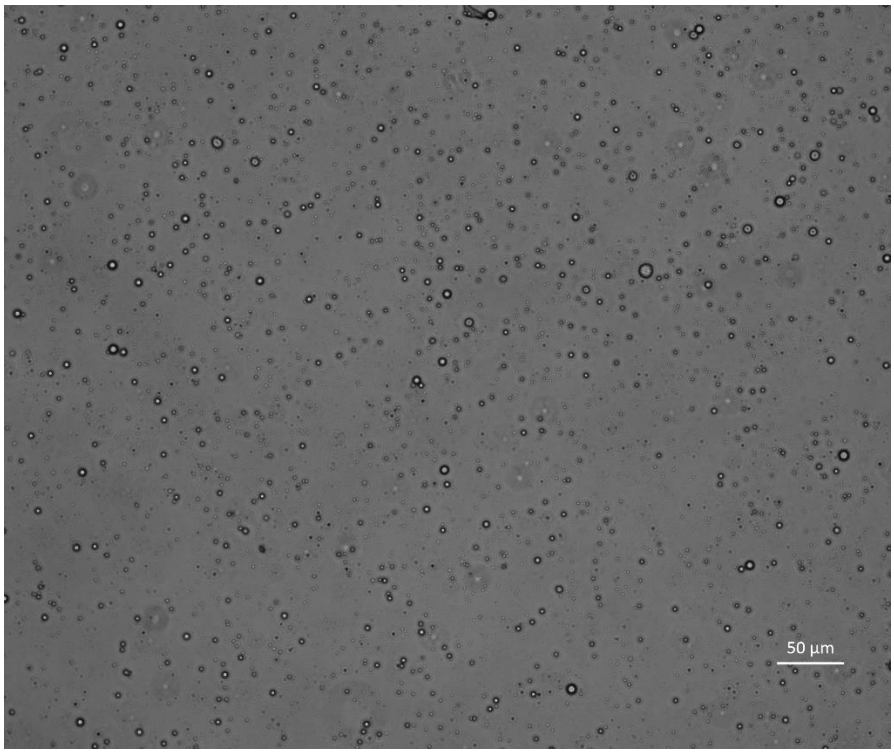

b)

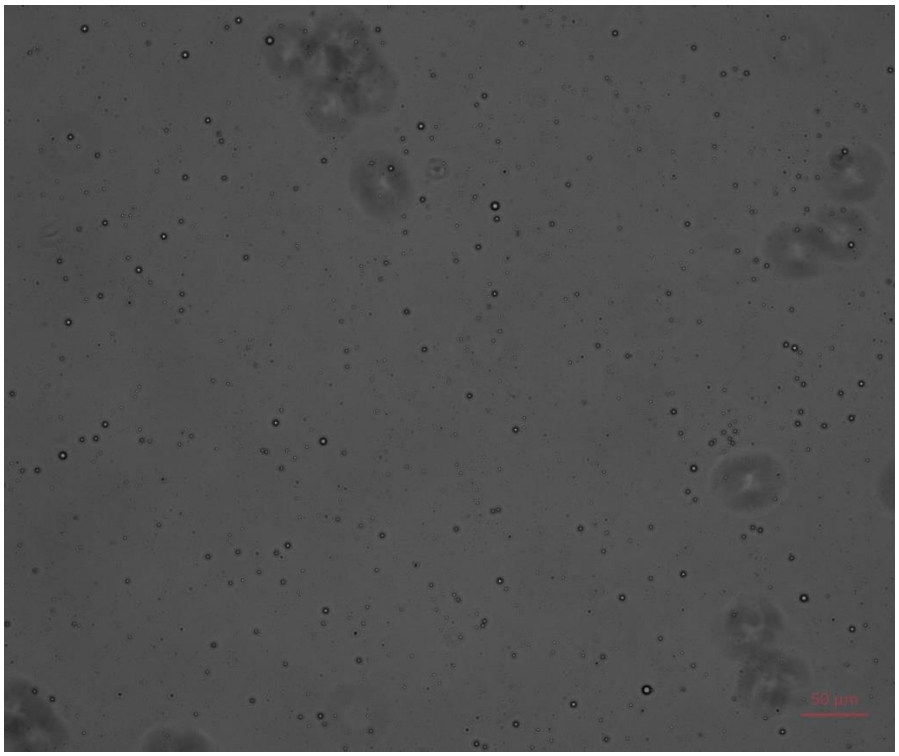

c)

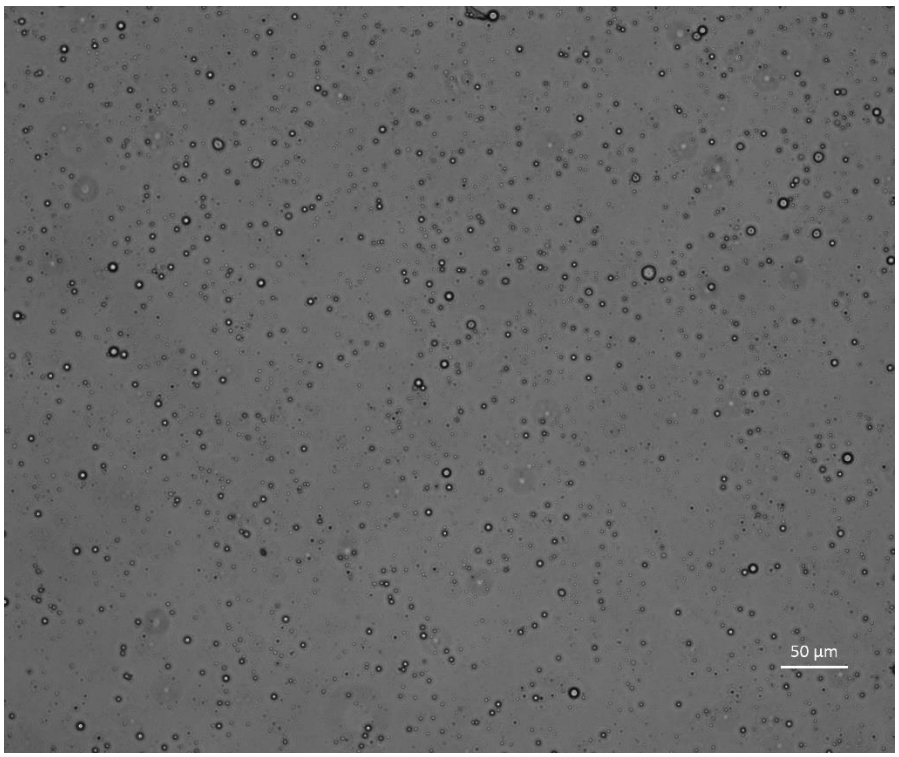

Figure 4.4 Microscope images of a) OWE-Tween 80, b) OWE-B, c) OWE-SDS

The optical microscope can visualize micrometer-sized droplets, while DLS shows droplets down to several nanometers. Among the three emulsions, OWE-B shows a monodisperse size distribution with an average droplet diameter of 512 (±14,5) nm in DLS. The optical microscope images for this emulsion also show a maximum droplet of diameter of 3,68 μm, with a lower concentration compared to the other emulsions. Also, the absence of such big droplet diameters in DLS implies that these are not the majority of the suspension. This is to be expected since boron oil is an industrial, well formulated product that should give stable, monodisperse emulsions when mixed with water.

The average droplet diameter measured is 135 (±12,7) nm via DLS and is 3,85 (±1,22) μm via optical microscopy for OWE-T80. OWE-SDS has a polydispersed droplet size distribution. The two highest intensity percent average droplet diameter sizes measured are 736 (±30,8) and 925 (±114) nm via DLS and is 3,21 (±1,86) μm via optical microscopy for OWE-SDS.

Thus, optical microscope was used prior to each filtration experiment for checking emulsion did not contain oil droplet bigger than 5 μm.

4.1.3 Membrane Performance Tests

4.1.3.1 Dead-end Filtrations

4.1.3.1.1 Surfactant Adsorption

OWE-Tween 80 filtrations were performed on flat PES membranes prior to hollow fiber ones. Membrane was placed in the dead-end cell and pure water permeance, filtration and pure water permeance after filtration were performed consecutively.

The feed emulsion was stirred in the cell during filtration. This cycle was repeated twice on a flat PES membrane. The permeance plot is given in Figure 4.5.

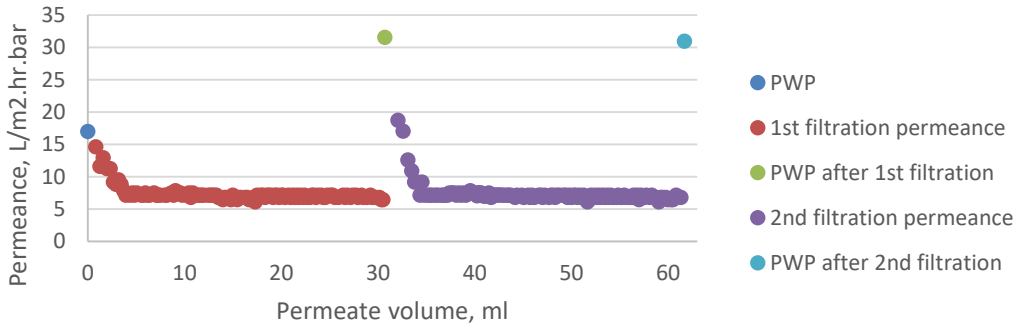

Figure 4.5 Permeance plot of OWE-Tween 80 filtration on flat PES membrane

As observed in Figure 4.5, PWP of the membrane increased after the 1st OWE filtration to a value higher than the initial PWP. After a 2nd filtration, the PWP again returned to this higher value. This may result from the adsorption of Tween 80 molecules in the emulsion onto the membrane surface and making the surface hydrophilic. In order to see whether the reason of the increase in PWP is the adsorption of Tween 80 molecules, 0,1 g/l Tween 80 solution was filtered on a virgin flat PES membrane. Permeance plot of PWP, 0,1 g/l Tween 80 solution filtration and PWP after the filtration is given in Figure 4.6. Same observation was made when only the surfactant solution was filtered through the membrane.

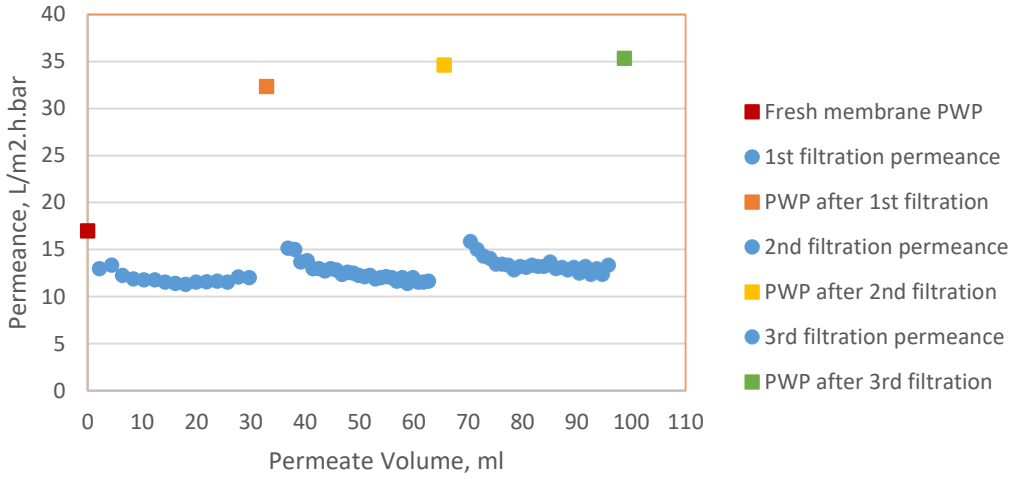

Figure 4.6 Permeance plot of 0,1 g/l Tween 80 filtration on flat PES membrane

It is clear that the PWP value raise after each filtration was caused from the adsorption of Tween 80 molecules. The adsorption of Tween 80 molecules can also be observed in ATR-FTIR analysis. The ATR-FTIR analysis was performed on a virgin and 0,1 g/l Tween 80 solution filtered membrane and Tween 80 itself given in Figure 4.7.

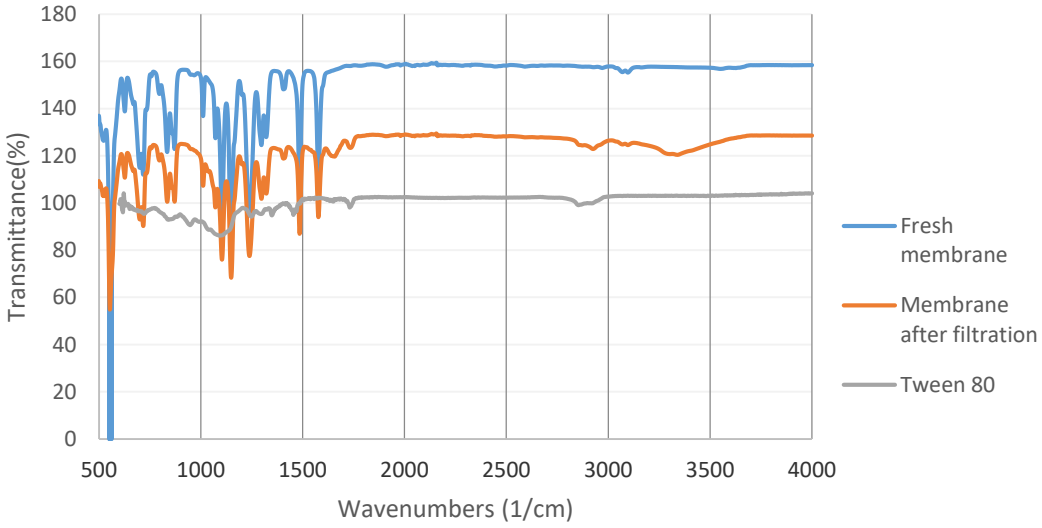

Figure 4.7 FTIR analysis on fresh membrane, membrane after 0,1 g/l Tween 80 solution and Tween 80 droplet.

It is seen that C=O group in Tween 80 molecule was observed on the membrane after filtration at 1730 cm-1 wavelength. Also, C-H group at 2864 cm-1 was detected on the membrane after filtration. Both C=O and C-H groups at the given wavelengths were not detected on the unused membrane before Tween 80 filtration.

After surfactant filtration, the surface becomes more hydrophilic due to the adsorption of Tween 80 molecules with their hydrophobic ends on hydrophobic PES surface and tailing their hydrophilic moiety to the aqueous environment (Holmberg et al., 2004). Consequently, membrane surface becomes more prone to water molecules and having an increased flux afterwards. (Xia et al., 2018)

As a result, it was decided to perform surfactant filtration as conditioning step to OWE filtration to ensure that fouling with oil droplets would be analyzed from the beginning of the OWE filtration, without the simultaneous surfactant adsorption.

4.1.3.2 Cross-flow Filtrations

Cross-flow filtrations were performed to investigate the effect of various membrane and process parameters on fouling behavior. While the dead-end filtrations were performed at a single pressure, cross-flow filtrations were performed at increasing values of pressure. The filtrations start at 0.3 bar, and continue to increase until the limiting flux is reached. Duration of filtrations at each different pressure is 30 minutes. After 30 minutes, pressure is increased by 0.2 bar increments.

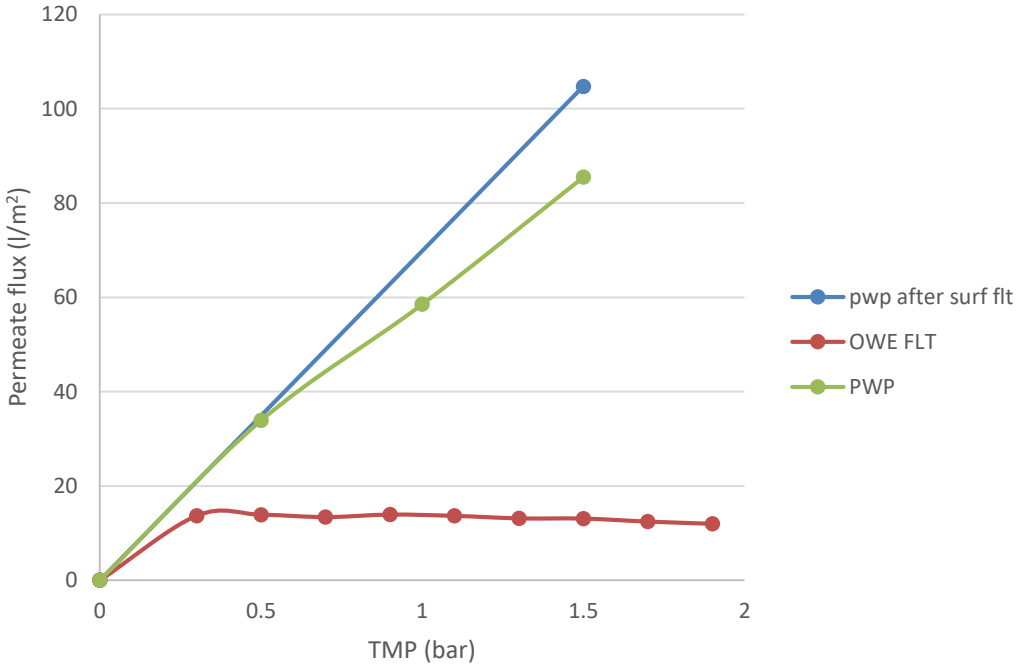

Figure 4.8 An example of cross-flow filtration via TMP step using OWE-Tween 80 on twisted membrane.

In Figure 4.8, the flux is seen to increase by increasing TMP. After limiting flux is reached, the flux becomes constant and further increase in the pressure and the filtration duration causes increasing deposition of droplets on the membrane surface.

The oil rejection was calculated according to the turbidity measurements of the permeate and the feed OWE. Turbidity measurements of samples and rejection values from one of the filtrations are given in Table 4.2.

Table 4.2 Turbidity and rejection values of samples from an OWE-Tween 80 filtration on twisted HF

Pressure, bar	**Permeate turbidity, NTU**	**Retantate turbidity, NTU**	**Rejection, %**
0,3	0,18	1434	99.99
0,5	0,18	1444	99.99

Tablo 4.2 (Cont'd)

0,7	0,09	1416	99.99
0,9	0,09	1408	99.99
1,1	0,14	1372	99.99
1,3	0,28	1328	99.98
1,5	0,31	1310	99.98
1,7	0,13	1318	99.99
1,9	0,16	1338	99.99

As seen from Table 4.2, the oil rejection values throughout the filtration were over 99,98%. Same rejection was observed for all filtrations. The separation performance of twisted membrane was exquisite. But, in order to achieve a sustainable and feasible membrane process, fouling has to be decreased and kept reversible. In order to decrease fouling, the effect of fiber geometry, cross-flow velocity, emulsion and membrane material were investigated.

4.1.3.2.1 Effect of Fiber Geometry

Spiral geometry of the hollow fibers disturbs the flow field and creates vortices near the membrane wall, which is expected to decrease concentration polarization and droplet deposition. (Ahmad & Mariadas, 2004)(Akagi et al., 2018)

In Figure 4.9 and 4.10, the limiting fluxes and fouling resistance values at 1,5 bar of the hollow fibers are given, respectively. 1,5 bar was chosen to compare all membranes as a representative value when it all cases the limiting flux was reached. Straight fibers having lower limiting fluxes and higher fouling resistance values at 1,5 bar show that straight fibers are more prone to fouling than the twisted fibers. When PWP loss% data given in Figure 4.10 are considered, it is seen that an average straight fiber recovered more of their initial PWP that twisted fibers did. So, twisted

fibers are less likely to foul but the fouling on twisted fibers is more irreversible than on straight fibers. It was mentioned before that twisted fibers have geometrical advantage during filtration, but this may be a drawback when filtering oil-water emulsions in which the oil droplets are deformable. Oil droplets deform under sufficient pressure (Tummons et al., 2016). Flow instabilities occurring in the spiral geometry may have a scouring effect on the membrane surface (Ahmad et al., 2004). As a result of this effect, some of the droplets may deform and cause internal fouling.

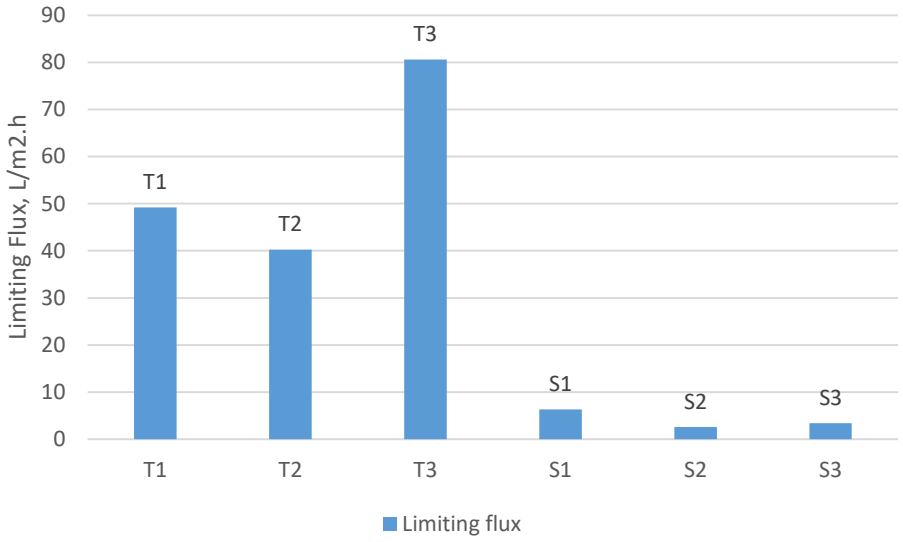

Figure 4.9 Limiting fluxes during OWE-Tween 80 filtration on twisted and straight membranes

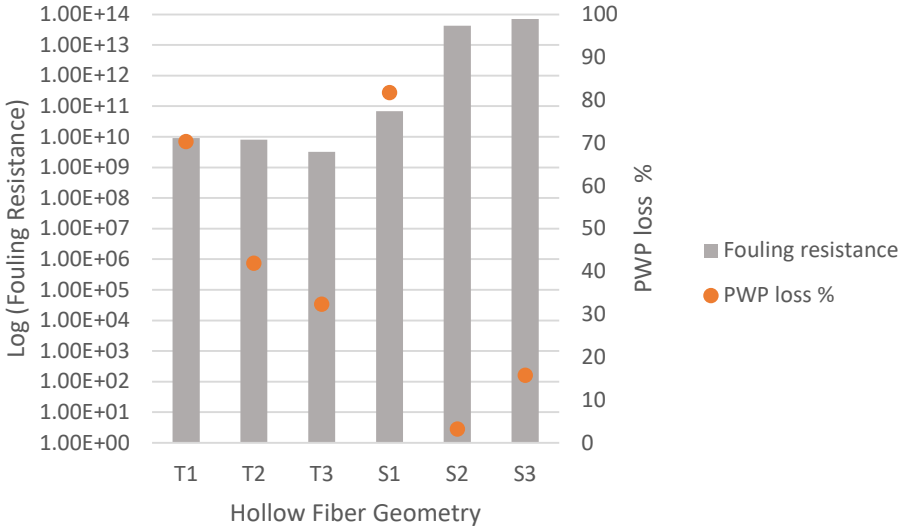

Figure 4.10 PWP loss % and fouling resistance at 1,5 bar during OWE-Tween 80 filtration on twisted and straight membranes

4.1.3.2.2 Effect of Cross Flow Velocity

As known, cross-flow filtration is preferred over dead-end filtration due to its nature of creating shear on the membrane surface.(Akagi et al., 2018)

However, fouling can still occur on the membrane. As known, the solute transferred from the bulk to the membrane surface by the convective flux is balanced by the diffusive flux of the solute from the membrane surface to the bulk. The retained solutes form a gel layer on the membrane surface if sufficient back diffusion of the solutes from the surface to the bulk cannot be supplied. Then, since the parameters in the mass balance equation (kc, co, cb) are fixed, flux becomes constant mathematically as limiting flux, Jlim. After the formation of gel layer, increasing TMP does not result in an increase in the flux.

$$Jlim = kc \ln\left(\frac{co}{cb}\right) \quad (9)$$

(Incropera et al., 2017)

where kc is the mass transfer coefficient, cb is the concentration of solute in the bulk (Baker, 2001). The limiting flux is directly proportional to the convective mass transfer coefficient, such that as the crossflow velocity is increased, or turbulence is promoted via surface structures, the mass transfer coefficient and the limiting flux are expected to increase.

As anticipated, the higher the cross-flow velocity, the higher the mass transfer coefficient thus the less the oil droplets accumulate on the membrane surface due to high shear and turbulence at the surface of the membrane. As a result, the limiting flux increases with the CFV. This was observed when Re was set to 401, 972 and 1404. Re was increased due to the increase in the cross flow velocity during OWE-Tween 80 filtrations on twisted hollow fiber membranes as seen in Figure 4.11.

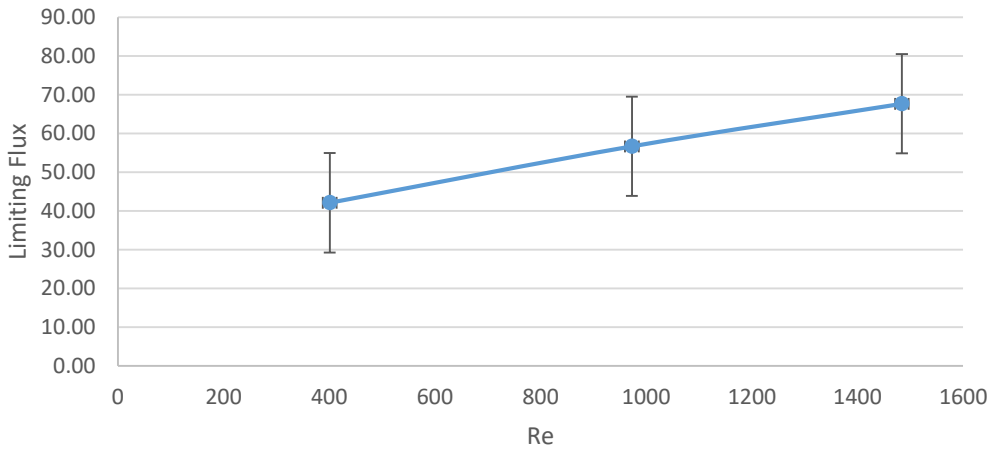

Figure 4.11 CFV effect on Limiting filtration flux for OWE-Tween 80 filtration on twisted membranes

CFV effect on fouling was also investigated with respect to PWP loss % and fouling resistance. As given in Figure 4.12, lesser values of PWP loss and fouling resistance were obtained for higher CFV. Higher CFV creating higher shear resulted in lower fouling as anticipated from fouling resistance values. Also, since the PWP loss%

values are lower for higher CFV, it can be said that the fouling occurring at higher CFV were more reversible than for lower CFV. This may be explained with the less dominant oil droplet-membrane interactions at higher CFVs (Zamani et al., 2016).

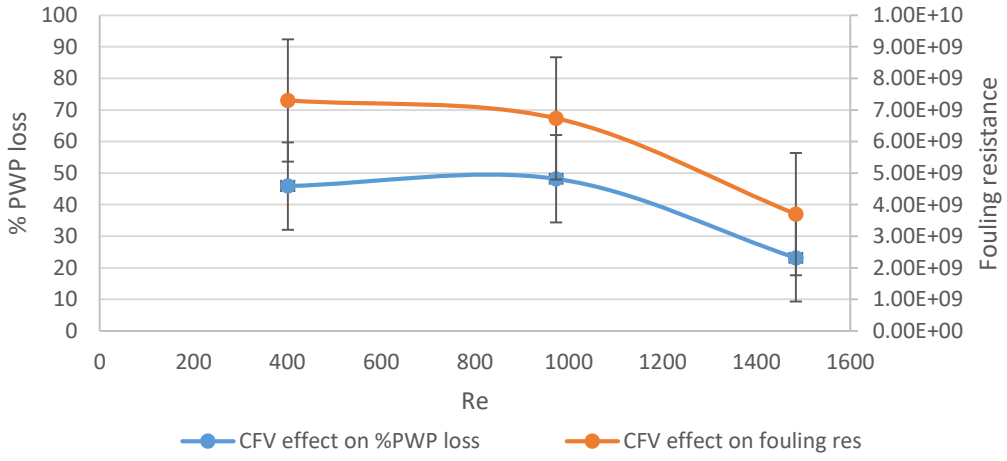

Figure 4.12 CFV effect on PWP loss % and fouling resistance at 1,5 bar during OWE-Tween 80 filtration on twisted membranes

4.1.3.2.3 Effect of Emulsion

Three different emulsion recipes were used to observe the effect of emulsifier on membrane fouling. OWE-Tween 80 and OWE-SDS differ by the surfactant. OWE-B, however, differs in both oil type and surfactant, and is an optimized commercial recipe, likely, with more components in addition to oil and surfactant. Tween 80 is a nonionic, while SDS is anionic surfactant. All emulsions were stable enough to prevent oil particles coalesce during the filtration. Among all, OWE-B was the most homogenous emulsion since boron oil is a commercial product, formulized well. Limiting flux data was given in Figure 4.13 and fouling resistance and PWP loss% are given in Figure 4.14. After each of these emulsions filtered from separate twisted membranes, each membrane was subjected to a back wash cleaning procedure where

UP water was filtered from the membranes in the opposite direction of OWE filtration, that was from inside to outwards. In that way, a second fouling removal strategy was applied to see how much fouling can be removed. A PWP loss% was calculated according to the PWP values after back wash cleaning procedure. Those values were also given in Figure 4.14.

OWE-B fouled less according to the limiting flux and fouling resistance given in both Figure 4.13 and 4.14. It may be caused from the monodispersity of the oil droplets in OWE-B that the fouling resistance is lower for the monodispersed droplets. Monodispersed droplets are more likely to be easily removed, also explaining the lower PWP loss%. After OWE-T80 and OWE-SDS filtrations, 70% PWP loss occurred in the membranes. Also, OWE-T80 caused slightly higher fouling resistance than OWE-SDS, but it was cleaned better than OWE-SDS. This can again be related to OWE-SDS polydispersed droplets. Polydispersed droplets are expected to form tighter cake layer than monodispersed ones, making the cake layer more irreversible. (Trzaskus et al., 2016)

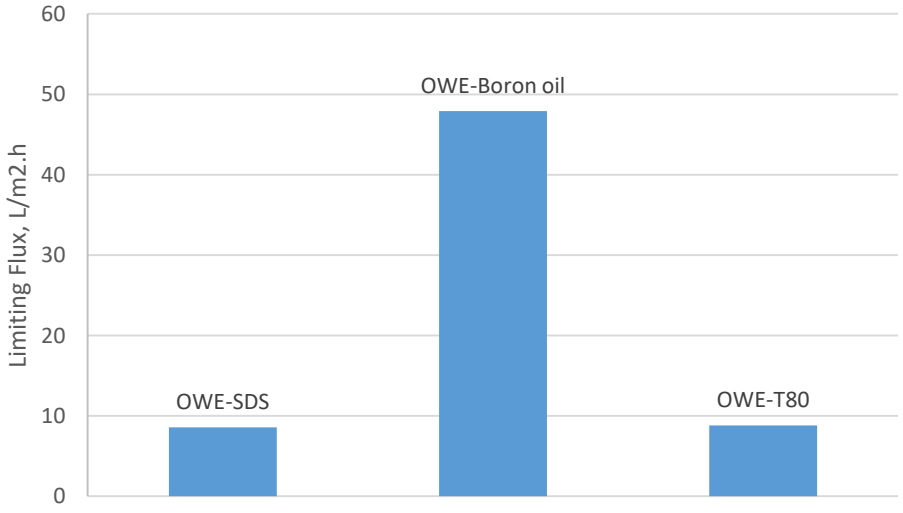

Figure 4.13 Limiting filtration flux for OWE-Tween 80, OWE-Boron oil and OWE-SDS filtration on twisted membranes

Figure 4.14 PWP loss %, fouling resistance at 1,5 bar and PWP loss % after back wash during OWE-Tween 80, OWE-Boron oil and OWE-SDS filtration on twisted membranes

After each of these emulsions filtered from separate twisted membranes, each membrane was subjected to a back wash cleaning procedure. In that way, the fouling on the surface of the membrane was aimed to be removed at some level. A PWP loss % was calculated according to the PWP values after back wash cleaning procedure. Those values were also given in Figure 4.14.

According to Figure 4.14, further cleaning achieved via back wash cleaning was not significant and was only slightly effective with OWE-B. As mentioned before, monodispersed droplets are easier to remove from the surface, thus, the reversibility of OWE-B fouling may be as a result of its monodispersed droplets. (Trzaskus et al., 2016)

4.1.3.2.4 Effect of Fiber Material

Until now all of the parameters were tested with PES hollow fibers. Although a common membrane material, in UF processes including oily water treatment, it is

known that PES is a hydrophobic material (contact angle ca. 65-80º), and in the use of oil-water emulsion, PES surfaces are prone to fouling if surface modifications are not made. (Manawi et al., 2017) (Rahimpour & Madaeni, 2010) On the other hand, cellulose acetate is a more hydrophilic polymer (contact angle ca. 39º) (Rajesh et al., 2011). To examine the material effect on the fouling, straight cellulose acetate and PES hollow fiber membranes were subjected to OWE-Tween 80 filtration. Membranes were cleaned via UP water without applying pressure after OWE-Tween 80 filtration. Limiting flux, PWP loss% and fouling resistance data are given in Figure 4.15 and 4.16. Limiting flux of CA membrane and the average of PES membranes were close due to same hydrodynamic conditions during filtrations. Even though, CA showed the highest fouling resistance during OWE-T80 filtration, the fouling on CA was the most reversible one as seen in PWP loss % data, implying that the interaction between CA membrane surface and oil droplets were not strong enough, and hence PWP of CA recovered better than PES membranes with cleaning just water.

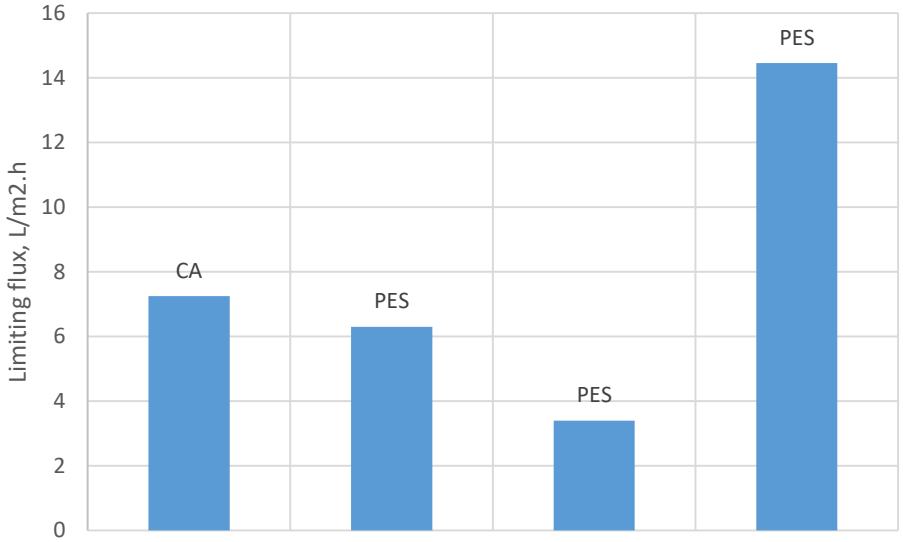

Figure 4.15 Limiting filtration flux for OWE-Tween 80 filtration on CA and three different PES straight membranes

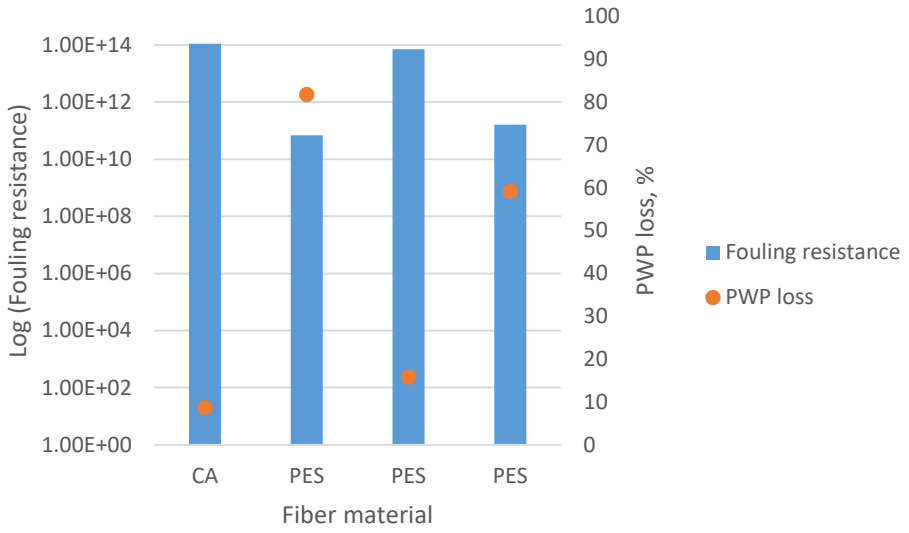

Figure 4.16 PWP loss % and fouling resistance at 1,5 bar during OWE-Tween 80 filtration on CA and three different PES straight membranes

To summarize, effect of various parameters on fouling were investigated. First of all, membrane geometry was found to be an effective parameter on fouling as spiral geometry disturbs the flow and creates higher shear that prevents oil droplets from fouling on the surface. In addition, increase in cross-flow velocity resulted in increase in mass transfer coefficient and limiting flux so fouling can be lowered by operating at cross-flow velocities high enough to increase limiting flux. Geometry and CFV effects studied previously are given in Table 4.3 with the data from this study.

Table 4.3 Previous and the current studies on the geometry and CFV effects

Reference condition	**Re**	**Baffle addition**	**Limiting flux increase, %**	
No baffle	68	Helical	56	(Akagi et al., 2018)
No baffle	Not specified	Helical 1 turns/50 mm	36,60	(Ahmad & Mariadas, 2004)

Table 4.3 (Cont'd)

	Not specified	Helical 2 turns/50 mm	55,80	(Ahmad & Mariadas, 2004)
	Not specified	Helical 4 turns/50 mm	104,90	(Ahmad & Mariadas, 2004)
	Not specified	Helical 6 turns/50 mm	27,80	(Ahmad & Mariadas, 2004)
	Not specified	Helical double helix	44,70	(Ahmad & Mariadas, 2004)
Straight HF	Not specified	Helical membrane	566	This study, geometry effect
Re=68	Re=200	-	22,22	(Akagi et al., 2018)
	Re=300	-	27,78	(Akagi et al., 2018)
	Re=400	-	29,63	(Akagi et al., 2018)
	Re=600	-	31,48	(Akagi et al., 2018)
Re=68, w/ helical baffle	Re=200	Helical	2,5	(Akagi et al., 2018)
	Re=600	Helical	4,25	(Akagi et al., 2018)
Re=419	Re=838	-	180	(Tanudjaja et al., 2017)
	Re=1255	-	300	(Tanudjaja et al., 2017)
	Re=1677	-	380	(Tanudjaja et al., 2017)
Re=401	Re=1484	Helical membrane	60,63	This study, CFV effect

According to the Table 4.3, it can be seen that previous studies agree with our data for both helical geometry and increase in CFV contributing to limiting flux incline.

It was mentioned before that increase in CFV results in higher shear in the membrane surface and increases back diffusion from the membrane surface and thus decreases concentration polarization. Helical baffles also create shear on the membrane surface in addition the mixing the bulk flow with the boundary layer which also resulting in a lesser concentration polarization. Helical baffles, or spiral geometry in this case, has advantage by creating turbulence compared to increase in CFV, since rapid flow without the turbulence, still creates uniform streamlines along the boundary layer which are not as effective mitigating concentration polarization.

Moreover, to see the effect of surfactant/oil/membrane interaction, 3 different emulsions were filtered, and OWE-B was found to foul less presumably due to its monodispersity while no remarkable difference was observed between OWE-T80 and OWE-SDS prepared with non-ionic and anionic surfactants, respectively. Finally, PES and CA as membrane materials were compared. Even though, hydrophilic property of CA cannot prevent the membrane from fouling under hydrodynamic conditions favoring deposition of oil droplets, it increased PWP recovery. PES membranes fouled and recovered less than CA.

4.2 EG Recovery from Aqueous EG- $NaHCO_3$ Solutions

Ethylene glycol recovery process used in this study aims at selectively permeating EG while rejecting $NaHCO_3$ via NF membrane. There were two streams where EG recovery was aimed. The composition and osmotic pressure of the streams are given in Table 4.4.

Table 4.4 Composition of the streams

Stream #	**$NaHCO_3$ concentration (%wt)**	**EG concentration (%wt)**	**Osmostic pressure at 30°C (bar)**
1	0.15	26	0.92
2	2.2	2.5	13

Three membranes were used for the filtrations. At first, filtrations were performed with solutions containing $NaHCO_3$ only prepared accordingly to the streams 1 and 2 as in Table 4.4.. A demonstrative plot of the sequential filtrations is given below.

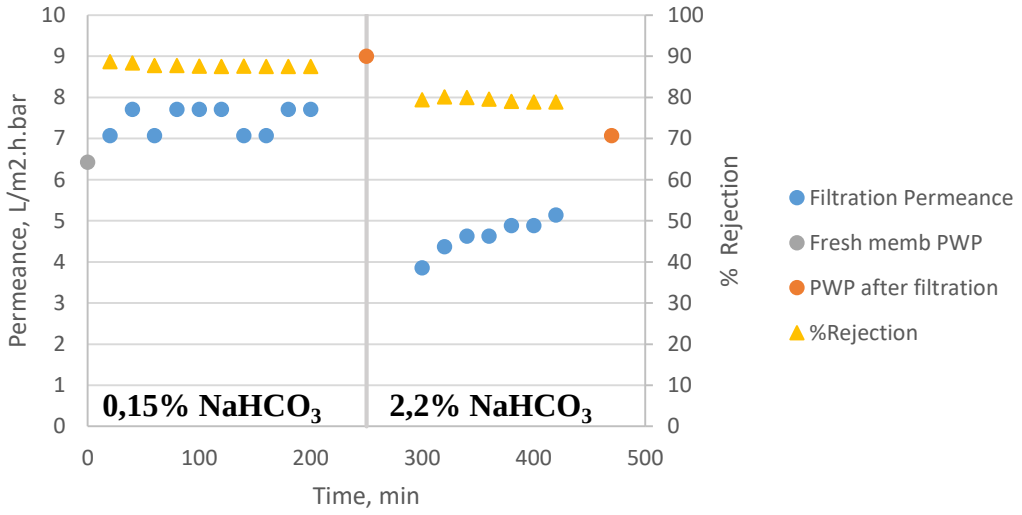

Figure 4.17 Permeance and salt rejection of Desal DK membrane during 0,15% and 2,2% $NaHCO_3$ filtrations respectively.

0,15% $NaHCO_3$ solution was filtered at 10 bar of TMP for 3 hours and then cleaned with UP water. After measuring PWP, membrane was subjected to 2,2% $NaHCO_3$ filtration at 25 bar of TMP. Then the cleaning procedure was repeated and PWP was measured. As can be seen in Figure 4.17, the DK membrane had higher salt rejection, around 87%, for the 0,15%-concentrated salt solution. The rejection values

decreased to 79% as the 2,2%-concentrated solution filtration started. High salt concentration also affected permeance values. In 0,15% salt filtration, PWP was around 7,5 L/m2.h.bar, whereas it decreased to 4,5 L/m2.h.bar when filtrating 2,2% salt solution. This is due to the decrease in the driving force (TMP-(Δπfeed-Δπpermeate)), that, increasing osmostic pressure of the feed solution resulted in decrease in the net applied pressure. Even though, the filtration permeance affected from the salt concentration, no irreversible fouling was seen on the membrane, as the initial PWP value was recovered at the end of the filtrations.

A set of synthetically prepared $NaHCO_3$ solution filtrations was performed on DK, DL and HL membranes. Each membrane was subjected to a 0,15% salt concentration solution and 2,2% salt concentration solution afterwards. The results of this set of experiments are given in Figure 4.18 and 4.19, respectively.

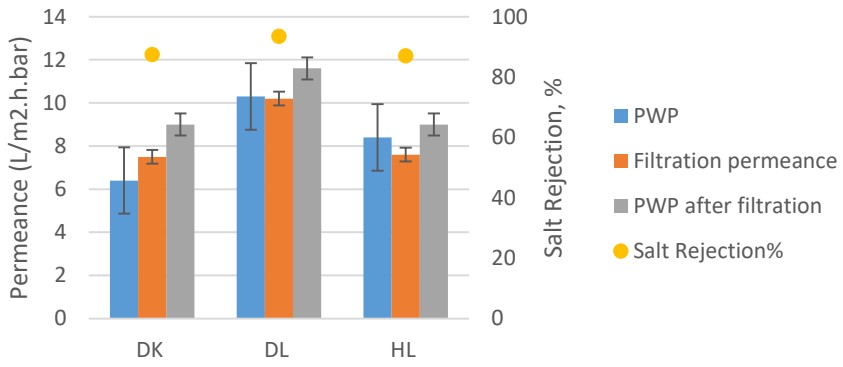

Figure 4.18 Filtration of 0,15% $NaHCO_3$ solutions on DESAL DK, DL and HL membranes in total recycle mode

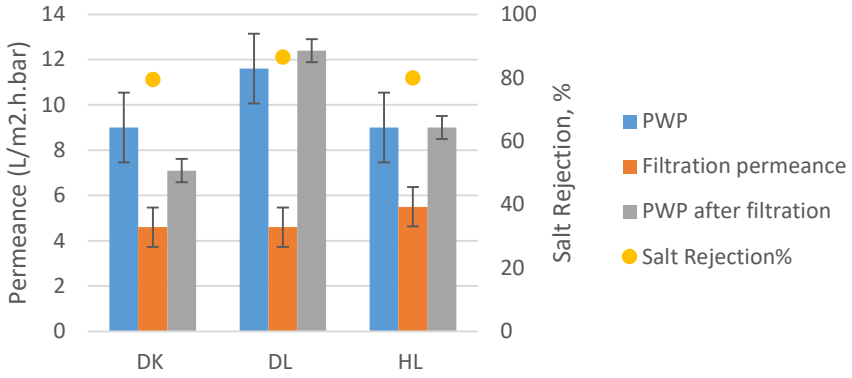

Figure 4.19 Filtration of 2,2% $NaHCO_3$ solutions on DESAL DK, DL and HL membranes in total recycle mode

For each membrane, it is obvious that each membrane had higher salt retention during 0,15% salt solution filtration (in Figure 4.18) than 2,2% salt solution filtration (in Figure 4.19). When filtration permeance values of 0,15% and 2,2% $NaHCO_3$ solutions filtrations are compared, permeance during 2,2% $NaHCO_3$ solution filtrations were seen to be decreased. For all 3 membranes, the decrease in retention and permeance are considered to be due to the concentration polarization as filtration permeance was lower than PWP but was stable throughout the filtration.

For 0,15% and 2,2% $NaHCO_3$ solution filtrations, DL had higher salt retention. The filtration permeance of DL was also higher than the others. All the membranes recovered well after the filtration via cleaning with water. This also supports the occurrence of concentration polarization as the major fouling contribution during the filtration.

After seeing the results of salt solution filtration tests, next step was to add EG to the system to see the effects of EG in salt filtration and to see whether it is possible to recover EG. EG retention was examined via TOC analysis for each filtration test and was found to be insignificant. To be representative, EG rejection of DK is given in Table 4.5 below.

Table 4.5 TOC analysis results for EG and EG retention of DK

Feed EG concentration,wt%/ TOC, ppm	Permeate-TOC,ppm	Retentate-TOC,ppm	EG Rejection, %
26/ 63.21			
	57.74	60.56	4.66
	56.33	63.83	11.75
	52.54	58.46	10.13
2.5/ 34.96	34.09	35.81	4.80
	34.65	26.56	-30.46
	42.11	39.76	-5.91

The $NaHCO_3$ rejection and permeance results of EG-$NaHCO_3$ solution filtrations on DK and DL membranes are given in Figure 4.20 and 4.21, respectively.

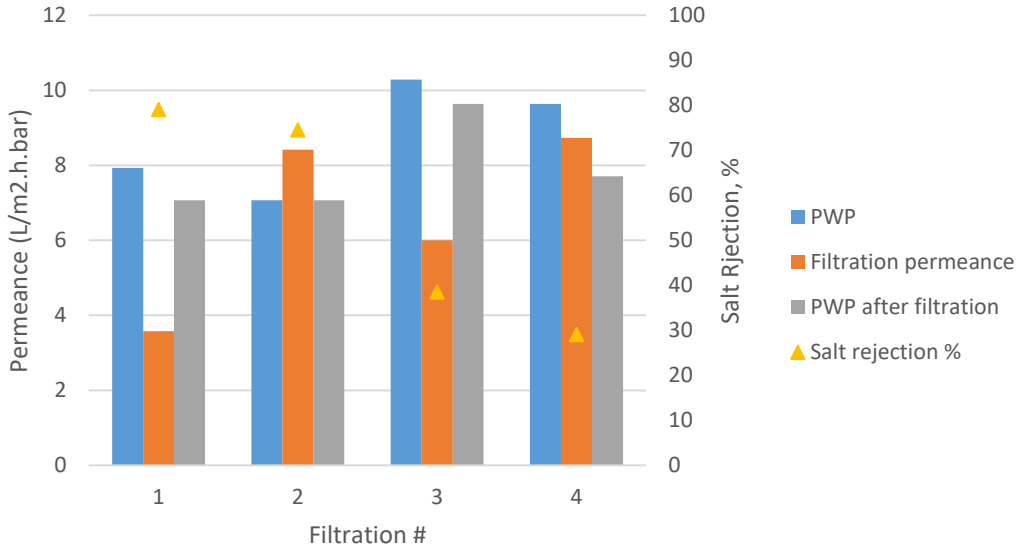

Figure 4.20 Filtration of 0,15% $NaHCO_3$ and 26% EG (filtration # 1 and 3) and 2,2% $NaHCO_3$ and 2,5% EG (filtration # 2 and 4) solutions on DESAL DK membrane in total recycle mode

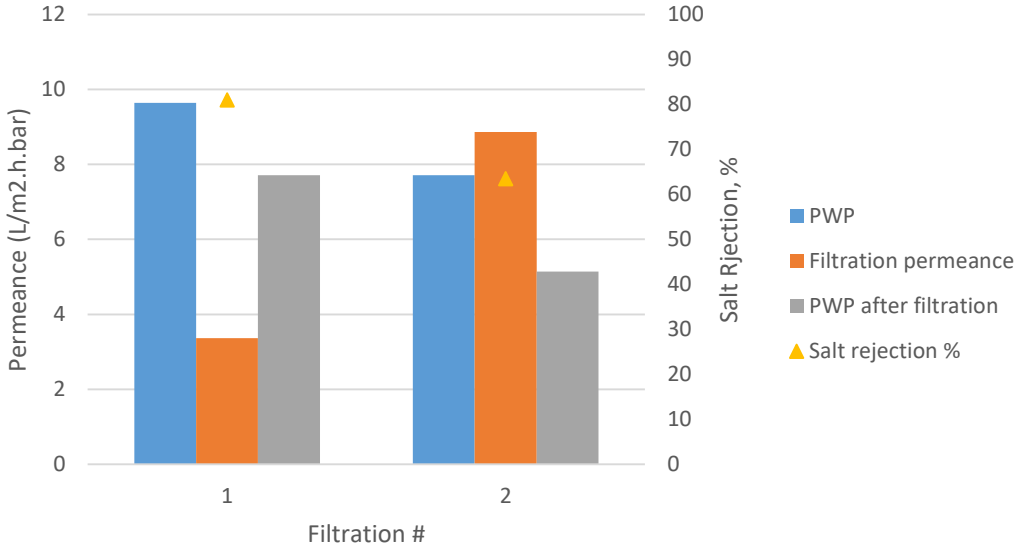

Figure 4.21 Filtration of 0,15% $NaHCO_3$ and 26% EG (filtration # 1) and 2,2% $NaHCO_3$ and 2,5% EG (filtration # 2) solutions on DESAL DL membrane in total recycle mode

In EG-salt filtrations, decreasing retention values in continuing filtrations were noticed after each 0,15% salt-26% EG solution filtration. Salt rejection of DK decreased from 79% to 38,5% after the exposure to high concentration EG solution during filtrations # 1 and 3 (in Figure 4.20), while DL retention decreased from 81% (filtration #1) to 63,5% (filtration #2) (in Figure 4.21). Since the only addition to the prior salt filtration experiments was EG, EG presence in the solution was examined. To understand its effect on the membrane, an aging experiment on DK membrane was performed for a month. Since its effect on DK is higher, DK membrane was kept in 26% EG solution for a month in between 2 filtration experiments. The plot of this 1-month aging experiment is given in Figure 4.22.

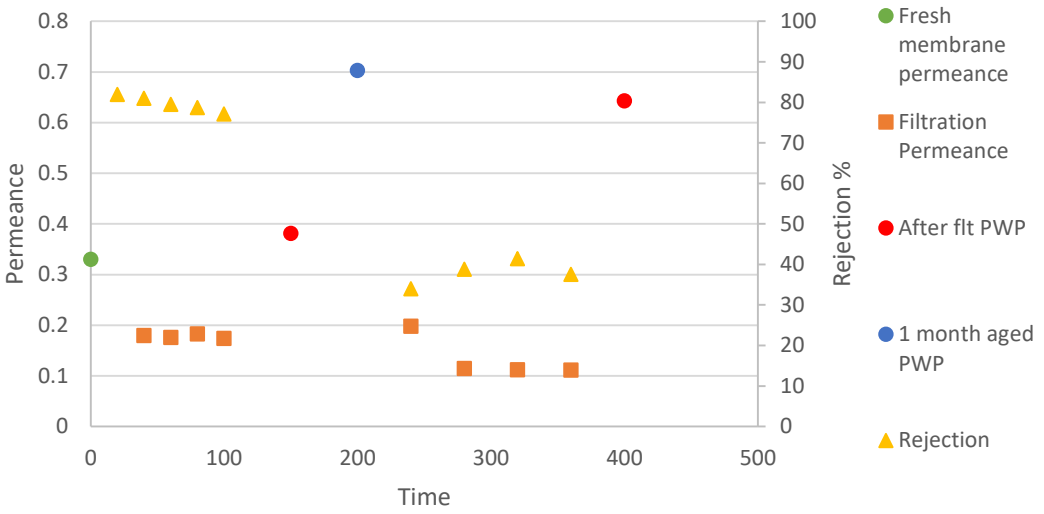

Figure 4.22 2,2% $NaHCO_3$- 2,5% EG filtration on DK membrane before and after aging in 26% EG solution for a month

Before kept in the 26% EG solution, the salt rejection of the membrane was around 80%, while after a month in EG solution, the salt rejection decreased to 38%. However, permeance values during filtration were not affected as much. The decay in the retention values may possibly be related to irreversible swelling and plasticizing of the membrane due to EG, so the pores of the membrane expanded in the presence of high EG concentration that higher number of salt molecules passed through the membrane. Also, pure water permeance value increased after aging in 26% EG solution that probably resulted inwider pore area.

Since the aim of the project was to recover EG from salty solutions, it was decided to continue with the higher salt- lower EG concentrated solution to eliminate the effect of high EG concentration on the salt retention. Therefore, 2,2% salt-2,5% EG solution was used in concentration mode filtration tests. These experiments were performed in concentration mode in which permeate was collected in a separate beaker, so that the feed solution was concentrated cumulatively. The results of concentration mode filtrations on DK and DL are given in Figure 4.23 and 4.24,

respectively. In concentration mode, DK was tested for 5 cycles and DL was tested for 6 cycles. In the beginning of each cycle, PWP was measured (red dots in the plots). Each filtration test (cycle) is separated with vertical guide lines.

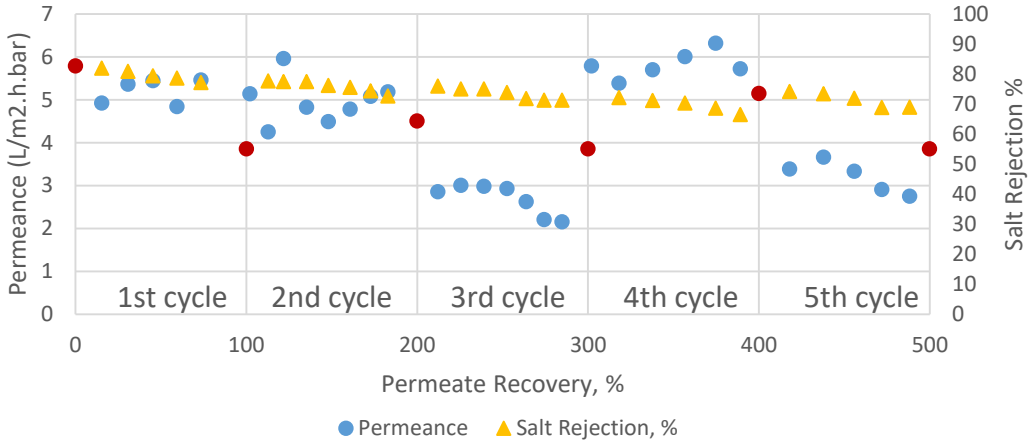

Figure 4.23 5 Sequential filtrations of 2,2% $NaHCO_3$- 2,5% EG solutions on DESAL DK membrane in concentration mode for 5 cycles

In concentration mode on DK (Figure 4.23), it is seen that filtration permeance decreases remarkably at the 3rd filtration cycle as a result of fouling.. However, even though the salt concentration increased by time, the lowest salt retention value was 66%, observed at the end of 4th cycle. In addition, since lower EG concentrated solution was used in filtrations, the significant decay in retention values mentioned above were not observed. This proves that the retention value decrease caused from high concentration EG in the solution.

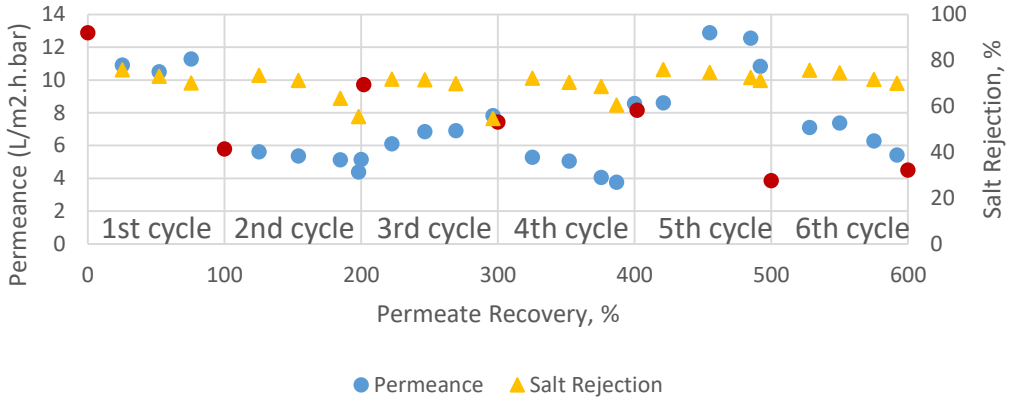

Figure 4.24 6 Sequential filtrations of stream 2 $NaHCO_3$-EG solutions on DESAL DL membrane in concentration mode for 6 cycles

In Figure 4.24, when PWP values before each filtration (red dots) are taken into account, it can be said that DL has lower fouling resistance than DK, since PWP values for DK were in a tighter range. The retention values are lower than DK. Both DK and DL have stable filtration permeance and salt retention values through the 1st and 2nd filtration cycles, which provides a starting point for EG recovery process design. Roughly, when the average $NaHCO_3$ rejection for DK is taken as 75%, and an average 80% of the feed volume is collected as permeate, and it contains 0,67% $NaHCO_3$ whereas the feed contains 2,2% $NaHCO_3$ in a single step membrane application. The average values of $NaHCO_3$ rejection and permeate recovery are taken according to Figure 4.23.

These experiments were performed to investigate whether EG recovery was possible by NF membranes. 1st stream was found to cause swelling on the membranes so EG recovery by membrane filtration was studied only on the 2nd stream. The average salt rejection was observed on DK at approximately 75%. With an 80% permeate recovery, salt concentration is decreased from 2,2% to 0,67%. For further desalination of the stream, a second DK membrane can be used. With 75% salt rejection and 80% permeate recovery assumptions, 64 L of 0,21% salt-2,5 % EG can recovered from a 2,2% salt-2,5% EG concentrated 100 L stream.

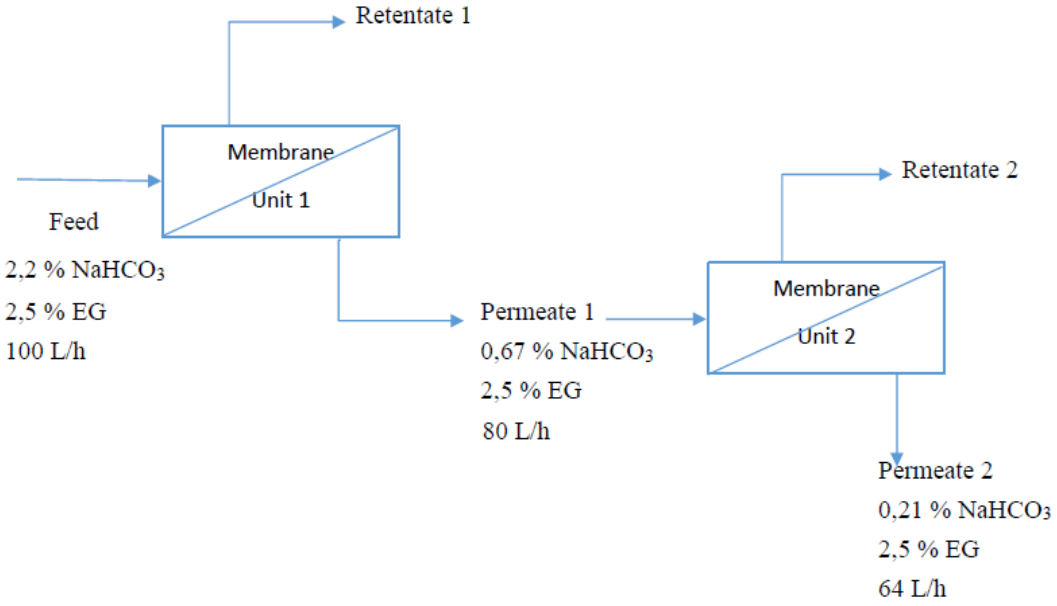

Figure 4.25 Process design for EG recovery by NF membranes

CHAPTER 5

CONCLUSION

In this study, two membrane separations relevant to the petrochemical industry were tested. The first one was to observe the effect of hollow fiber geometry, cross-flow velocity, emulsion type and membrane material on membrane fouling during OWE filtrations. Emulsions were prepared with sun flower oil-Tween 80, sun flower oil-SDS, and a commercial boron oil. All emulsions contained 1 g/l oil with oil droplet size less than 5 μm. The filtrations performed with a cross-flow system. The membranes used in the filtrations were straight and helical hollow fibers made out of PES or straight CA hollow fibers. Because of the fouling during the filtration, hollow fiber geometries were compared. Also, the effects of cross-flow velocity, type of emulsions and membrane material on fouling were observed. Spiral fiber geometry was found to foul less and more reversibly compared to the straight HF due to the flow instabilities and turbulance created by the spiral geometry. Increase in the cross-flow velocity resulted in less and reversible fouling because of the increased mass transfer of foulants from the membrane surface to the bulk flow. Emulsion oil droplet size distrubution was found to be important for the reversibility of the fouling. A monodispersed droplet sized emulsion such as OWE-B was observed to fouled more reversibly then the other two emulsions. According to membrane material, even though CA-made membrane fouled more and more reversibly than PES membrane due to CA's hydrophilic property.

In addition, EG and $NaHCO_3$ containing aqueous solutions were treated via three commercial nanofiltration (NF) membrane in a cross-flow system to retain the salt content and obtain a second grade EG product. The rejection values of DK and DL

membranes for $NaHCO_3$ were around 70 % during concentration mode filtrations with a feed of 2,2 % $NaHCO_3$ and 2,5 % EG. A membrane process was considered from the membrane performance results. It was found that the $NaHCO_3$ coontent of a feed containing 2,2 % $NaHCO_3$ and 2,5 % EG can be retained to provide a final product composed of 0,22 % $NaHCO_3$ and 2,5 % EG with a two stage Desal DK membrane process.

.

REFERENCES

Ahmad, A. L., & Mariadas, A. (2004). Baffled microfiltration membrane and its fouling control for feed water of desalination. *Desalination*, *168*(1–3), 223–230. https://doi.org/10.1016/j.desal.2004.07.002

Ahmad, A. L., Mariadas, A., & Zulkali, M. M. D. (2004). Reduction of membrane fouling using a helical baffle for cross flow microfiltration. *Regional Symposium on Membrane Science and Technology*.

Akagi, T., Horie, T., Masuda, H., Matsuda, K., Matsumoto, H., Ohmura, N., & Hirata, Y. (2018). Improvement of separation performance by fluid motion in the membrane module with a helical baffle. *Separation and Purification Technology*, *198*, 52–59. https://doi.org/10.1016/j.seppur.2017.07.012

Alenazi, N. A., Hussein, M. A., Alamry, K. A., & Asiri, A. M. (2017). Modified polyether-sulfone membrane: A mini review. *Designed Monomers and Polymers*, *20*(1), 532–546. https://doi.org/10.1080/15685551.2017.1398208

Baker, R. W. (2001). Membrane Technology. *Encyclopedia of Polymer Science and Technology*. https://doi.org/10.1002/0471440264.PST194

Benyahia, F., Abdulkarim, M., Embaby, A., & Rao, M. (2016). Refinery Wastewater Treatment: A true Technological Challenge. *In The Seventh Annual UAE University Research Conference. UAE University*.

Biancari, A., Di Palma, L., Ferrantelli, P., & Merli, C. (2003). Ethylene glycol recovery from dilute aqueous solution. *Environmental Engineering Science*, *20*(2), 103–110. https://doi.org/10.1089/109287503763336539

Bouchoux, A., Roux-de Balmann, H., & Lutin, F. (2006). Investigation of nanofiltration as a purification step for lactic acid production processes based on conventional and bipolar electrodialysis operations. *Separation and*

Purification Technology, *52*(2), 266–273. https://doi.org/10.1016/j.seppur.2006.05.011

Braeken, L., Bettens, B., Boussu, K., Van der Meeren, P., Cocquyt, J., Vermant, J., & Van der Bruggen, B. (2006). Transport mechanisms of dissolved organic compounds in aqueous solution during nanofiltration. *Journal of Membrane Science*, *279*(1–2), 311–319. https://doi.org/10.1016/j.memsci.2005.12.024

Chen, G., & Tao, D. (2005). An experimental study of stability of oil-water emulsion. *Fuel Processing Technology*, *86*(5), 499–508. https://doi.org/10.1016/j.fuproc.2004.03.010

Fane, A. G., Xi, W., & Rong, W. (2006). Chapter 7: Membrane filtration processes and fouling. *Interface Science and Technology*, *10*(C), 109–132. https://doi.org/10.1016/S1573-4285(06)80076-1

Fikar, M. (2014). Modelling, control, and optimisation of membrane processes. *Proceedings of the 2014 15th International Carpathian Control Conference, ICCC 2014*, 109–114. https://doi.org/10.1109/CarpathianCC.2014.6843579

Gorouhi, E., Sadrzadeh, M., & Mohammadi, T. (2006). Microfiltration of oily wastewater using PP hydrophobic membrane. *Undefined*, *200*(1–3), 319–321. https://doi.org/10.1016/J.DESAL.2006.03.323

Harmsen, J., & Verkerk, M. (2020). 15 Shell OMEGA only monoethylene glycol advanced process. *Process Intensification*, 166–175. https://doi.org/10.1515/9783110657357-015

Holmberg, K., Jönsson, B., Kronberg, B., & Lindman, B. (2004). Surfactant Micellization. In *Surfactants and Polymers in Aqueous Solution*. https://doi.org/10.1002/0470856424.ch2

Hu, B., & Scott, K. (2008). Microfiltration of water in oil emulsions and evaluation of fouling mechanism. *Chemical Engineering Journal*, *136*(2–3), 210–220.

https://doi.org/10.1016/j.cej.2007.04.003

Huang, S., Ras, R. H. A., & Tian, X. (2018). Antifouling membranes for oily wastewater treatment: Interplay between wetting and membrane fouling. *Current Opinion in Colloid and Interface Science*, *36*, 90–109. https://doi.org/10.1016/j.cocis.2018.02.002

Incropera, F. P., DeWitt, D. P., Bergman, T. L., & Lavine, A. S. (2017). Incropera's principles of heat and mass transfer. *Wiley*, 564. https://www.wiley.com/en-sg/Incropera%27s+Principles+of+Heat+and+Mass+Transfer%2C+8th+Edition%2C+Global+Edition-p-9781119382911

Kim, S., Ozaki, H., & Kim, J. (2006). Effect of pH on the rejection of inorganic salts and organic compound using nanofiltration membrane. *Korean Journal of Chemical Engineering 2006 23:1*, *23*(1), 28–33. https://doi.org/10.1007/BF02705688

Liang, Y., Ning, Y., Liao, L., & Yuan, B. (2018). Special Focus on Produced Water in Oil and Gas Fields : Origin , Management , and Reinjection Practice. In *Formation Damage during Improved Oil Recovery*. Elsevier Inc. https://doi.org/10.1016/B978-0-12-813782-6.00014-2

Liu, L., Li, L., Ding, Z., Ma, R., & Yang, Z. (2005). Mass transfer enhancement in coiled hollow fiber membrane modules. *Journal of Membrane Science*, *264*(1–2), 113–121. https://doi.org/10.1016/j.memsci.2005.04.035

Lobo, A., Cambiella, Á., Benito, J. M., Pazos, C., & Coca, J. (2006). Ultrafiltration of oil-in-water emulsions with ceramic membranes: Influence of pH and crossflow velocity. *Journal of Membrane Science*, *1–2*(278), 328–334. https://doi.org/10.1016/J.MEMSCI.2005.11.016

Luo, J., & Wan, Y. (2011). Effect of highly concentrated salt on retention of

organic solutes by nanofiltration polymeric membranes. *Journal of Membrane Science*, *372*(1–2), 145–153. https://doi.org/10.1016/j.memsci.2011.01.066

Manawi, Y., Kochkodan, V., Mahmoudi, E., Johnson, D. J., Mohammad, A. W., & Atieh, M. A. (2017). Characterization and Separation Performance of a Novel Polyethersulfone Membrane Blended with Acacia Gum. *Scientific Reports*, *7*(1), 1–12. https://doi.org/10.1038/s41598-017-14735-9

Monfared, M. A., Kasiri, N., & Mohammadi, T. (2016). Microscopic modeling of critical pressure of permeation in oily waste water treatment via membrane filtration. *RSC Advances*, *6*(75), 71744–71756. https://doi.org/10.1039/C6RA12266C

Olajire, A. A. (2020). Recent advances on the treatment technology of oil and gas produced water for sustainable energy industry-mechanistic aspects and process chemistry perspectives. *Chemical Engineering Journal Advances*, *4*(October), 100049. https://doi.org/10.1016/j.ceja.2020.100049

Pearce, G. (2007). Introduction to membranes: Membrane selection. *Filtration and Separation*, *44*(3), 35–37. https://doi.org/10.1016/S0015-1882(07)70083-6

Rahimpour, A., & Madaeni, S. S. (2010). Improvement of performance and surface properties of nano-porous polyethersulfone (PES) membrane using hydrophilic monomers as additives in the casting solution. *Journal of Membrane Science*, *360*(1–2), 371–379. https://doi.org/10.1016/j.memsci.2010.05.036

Rajesh, S., Shobana, K. H., Anitharaj, S., & Mohan, D. R. (2011). Preparation, morphology, performance, and hydrophilicity studies of poly(amide-imide) incorporated cellulose acetate ultrafiltration membranes. *Industrial and Engineering Chemistry Research*, *50*(9), 5550–5564. https://doi.org/10.1021/ie1019613

Singh, R. (2015). Introduction to Membrane Technology. *Membrane Technology and Engineering for Water Purification*, 1–80. https://doi.org/10.1016/b978-0-444-63362-0.00001-x

Tanudjaja, H. J., Tarabara, V. V., Fane, A. G., & Chew, J. W. (2017). Effect of cross-flow velocity, oil concentration and salinity on the critical flux of an oil-in-water emulsion in microfiltration. *Journal of Membrane Science*, *530*(December 2016), 11–19. https://doi.org/10.1016/j.memsci.2017.02.011

Trzaskus, K., Elshof, M., Kemperman, A., & Nijmeijer, K. (2016). Understanding the role of nanoparticle size and polydispersity in fouling development during dead-end microfiltration. *Journal of Membrane Science*, *516*, 152–161. https://doi.org/10.1016/j.memsci.2016.05.043

Tummons, E. N., Tarabara, V. V., Chew, J. W., & Fane, A. G. (2016). Behavior of oil droplets at the membrane surface during crossflow microfiltration of oil-water emulsions. *Journal of Membrane Science*, *500*, 211–224. https://doi.org/10.1016/j.memsci.2015.11.005

Um, M. J., Yoon, S. H., Lee, C. H., Chung, K. Y., & Kim, J. J. (2001). Flux enhancement with gas injection in crossflow ultrafiltration of oily wastewater. *Water Research*, *35*(17), 4095–4101. https://doi.org/10.1016/S0043-1354(01)00155-5

Vatai, G. N., Krstic, D. M., Höflinger, W., & Koris, A. K. (2007). *Combining air sparging and the use of a static mixer in cross-flow ultrafiltration of oil / water emulsion*. *204*(May 2006), 255–264. https://doi.org/10.1016/j.desal.2006.02.034

Xia, L., Vemuri, B., Saptoka, S., Shrestha, N., Chilkoor, G., Kilduff, J., & Gadhamshetty, V. (2018). Antifouling membranes for bioelectrochemistry applications. In *Biomass, Biofuels, Biochemicals: Microbial Electrochemical Technology: Sustainable Platform for Fuels, Chemicals and Remediation*.

Elsevier B.V. https://doi.org/10.1016/B978-0-444-64052-9.00008-X

Yoon, Y., & Lueptow, R. M. (2005). Removal of organic contaminants by RO and NF membranes. *Journal of Membrane Science*, *261*(1–2), 76–86. https://doi.org/10.1016/j.memsci.2005.03.038

Yücel, H., & Çulfaz-Emecen, P. Z. (2018). Helical hollow fibers via rope coiling: Effect of spinning conditions on geometry and membrane morphology. *Journal of Membrane Science*, *559*, 54–62. https://doi.org/10.1016/J.MEMSCI.2018.04.048

Zamani, F., Ullah, A., Akhondi, E., Tanudjaja, H. J., Cornelissen, E. R., Honciuc, A., Fane, A. G., & Chew, J. W. (2016). Impact of the surface energy of particulate foulants on membrane fouling. *Journal of Membrane Science*, *510*, 101–111. https://doi.org/10.1016/j.memsci.2016.02.064

Zhao, X., Zhang, R., Liu, Y., He, M., Su, Y., Gao, C., & Jiang, Z. (2018). Antifouling membrane surface construction: Chemistry plays a critical role. *Journal of Membrane Science*, *551*(92), 145–171. https://doi.org/10.1016/j.memsci.2018.01.039

APPENDICES

A. Permeate Flux Calculations

Straight Hollow Fiber Membrane

Effective Area Calculation

$$A = \pi\ Do\ L = \pi.\left(1307\ \mu m * 10^{-6}\frac{m}{\mu m}\right).(0{,}105\ m)$$

$$L = Ltube$$

$$A = \pi.\left(1307\ \mu m * 10^{-6}\frac{m}{\mu m}\right).(0{,}105\ m)$$

$$A = 4{,}3 * 10^{-4} m^2$$

ΔV = 0,098 ml/min at 1,5 bar

$$J = \frac{\Delta V}{A} = \frac{\left(0{,}098\frac{ml}{min}\right)\left(\frac{1\ L}{1000\ ml}\right)\left(\frac{60\ min}{1\ h}\right)}{4{,}3 * 10^{-4} m^2}$$

$$J = 13{,}67\ {}^{L}/_{h.m^2}$$

$$PWP = \frac{J}{TMP} = \frac{13{,}67\ L/h.m^2}{1{,}5\ bar}$$

$$PWP = 9{,}12\ {}^{L}/_{h.m^2.bar}$$

Twisted Hollow Fiber Membrane

Effective Area Calculation

$A = \pi\ Do\ L$

$L = 2Ltube$

$A = \pi.\left(1088\ \mu m * 10^{-6}\frac{m}{\mu m}\right).(2 * 0{,}105\ m)$

$A = 7{,}2 * 10^{-4} m^2$

ΔV = 0,31 ml/min at 1,5 bar

$$J = \frac{\Delta V}{A} = \frac{\left(0{,}31\frac{ml}{min}\right)\left(\frac{1\ L}{1000\ ml}\right)\left(\frac{60\ min}{1\ h}\right)}{7{,}2 * 10^{-4} m^2}$$

$J = 25{,}83\ {}^{L}/_{h.m^2}$

$$PWP = \frac{J}{TMP} = \frac{25{,}83\ L/h.m^2}{1{,}5\ bar}$$

$PWP = 17{,}22\ {}^{L}/_{h.m^2.bar}$

B. Reynolds Number Calculation

Volumetric Flow Rate

Calibration curve equation for the pump: $y = 1{,}0609x - 0{,}5341$

x= 104 rpm

$y = 1{,}0609 * 181 - 0{,}5341$

$y = 109{,}8\ \frac{ml}{min} = 1{,}83 * 10^{-6}\ {m^3}/{s} = Q$

Effective Area

$$Ac = \frac{Vf}{Ltube} = \frac{\left(\frac{\pi\ Dtube^2 Ltube}{4}\right) - \left(\frac{\pi\ Do^2 Lfiber}{4}\right)}{Ltube}$$

$Lfiber = 2Ltube$ for twisted HF

$$Ac = \frac{\pi(Dtube^2 - 2Do^2)}{4} = \frac{\pi\ ((4 * 10^{-3}m)^2 - 2\ (1{,}088 * 10^{-3}m)^2)}{4}$$

$Ac = 1{,}07 * 10^{-5}m^2$

Hydraulic Diameter

$$D_h = \frac{4\,A_C}{P_W} = \frac{4\,\pi\,\left(\frac{Dtube^2 - Do^2}{4}\right)}{\pi\,(Dtube - Do)}$$

$$Dh = \frac{(4000\,\mu m)^2 - (1088\,\mu m)^2}{4000\,\mu m - 1088\,\mu m} = 5088\,\mu m$$

$$Re = \frac{Q\,Dh}{\Upsilon\,Ac} = \frac{\left(1{,}83 * 10^{-6}\ {}^{m^3}/_{s}\right)(5088 * 10^{-6}\,m)}{\left(0{,}893 * 10^{-6}\,{}^{m^2}/_{s}\right)\ (1{,}07 * 10^{-5} m^2)}$$

$$Re = 974$$

C. Calibration Curves

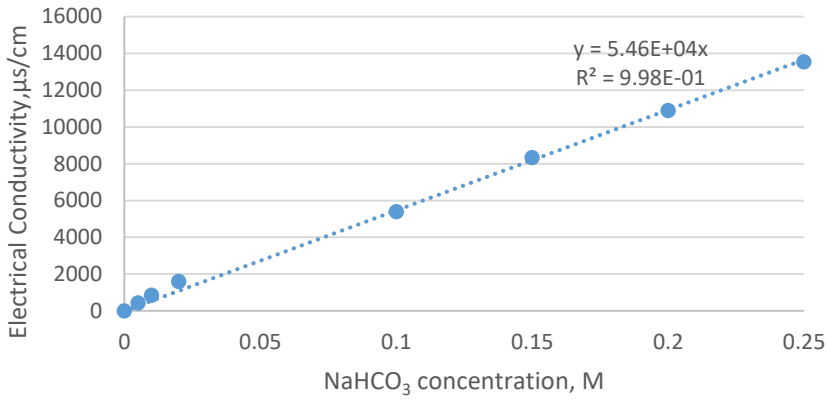

Figure B. 3 Calibration curve of $NaHCO_3$ concentration by Conductivitymeter in H2O

$$c_{NaHCO3}, M = \frac{\sigma, \mu s/cm}{54600}$$

To find out the calibration curve for $NaHCO_3$ concentration, $NaHCO_3$-H_2O solutions were prepared with concentrations of 0, 0.005, 0.01, 0.02, 0.1, 0.15, 0.2, 0.25 M. Conductivity values were measured three times for each solution. Average conductivity values for each solution were used for the plot of the calibration curve.

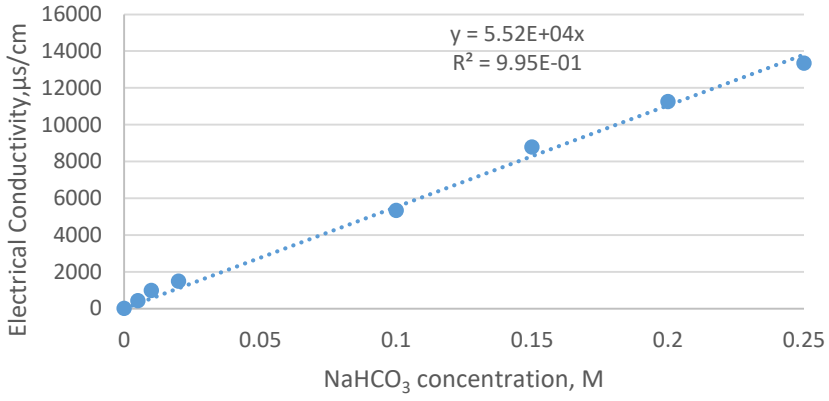

Figure B. 4 Calibration curve of $NaHCO_3$ concentration by Conductivitymeter in 2.5% EG solution

$$c_{NaHCO3}, M = \frac{\sigma, \mu s/cm}{55200}$$

Same procedure above was followed with 2.5% EG-H_2O solutions. $NaHCO_3$ concentration of the solutions were same as above. Conductivity values were measured three times for each solution. Average values were used for the plot of the calibration curve.